

# Upgrade of the H1 Forward Proton Spectrometer.

Inter-University ULB-VUB, Brussels  
DESY Hamburg  
University Hamburg II Institut f. Experimentalphysik  
University Kiel  
School of Physics and Materials, University Lancaster  
Lebedev Physics Institut Moscow  
CPPM, University Aix-Marseille  
Nuclear Center, Charles University, Prague  
INFN Roma Dipartimento di Fisica, La Sapienza Roma  
DESY Institut f. Hochenergiephysik Zeuthen

December 15<sup>th</sup> 1995

## Abstract

The data taken in 1995 with the H1 forward proton spectrometer show that it performs as anticipated in the technical proposal. It is proposed to upgrade the FPS by adding two new stations, which approach the circulating beam horizontally at 63 m and 80 m from the interaction point. Furthermore it is proposed to improve the spatial resolution of the present set up by adding Silicon-pixel detectors.

# Contents

<b>1</b>	<b>Introduction</b>	<b>3</b>
<b>2</b>	<b>Performance of the FPS During the 1995 Running Period</b>	<b>4</b>
<b>3</b>	<b>The Physics Case for an Upgrade of the FPS</b>	<b>9</b>
3.1	Horizontal Stations at 63 and 80 m . . . . .	9
3.1.1	Resolution . . . . .	12
3.2	Upgrade with Si-Pixel Detectors . . . . .	12
3.2.1	Intrinsic Pixel Detector Resolution and Efficiencies . . . . .	16
3.3	Impact of the 90 m Vertical Pot Instrumentation . . . . .	17
3.4	Impact of the Complete Instrumentation with Si-Pixels . . . . .	17
<b>4</b>	<b>Technical Description of the Upgraded FPS</b>	<b>17</b>
4.1	Fiber Detector . . . . .	17
4.1.1	Optoelectronic Readout . . . . .	20
4.1.2	The Trigger . . . . .	22
4.1.3	Mechanical Precision . . . . .	23
4.1.4	Read-Out Electronics . . . . .	23
4.2	The HERA Si-Pixel Detectors . . . . .	23
4.2.1	Radiation Levels . . . . .	23
4.2.2	Electronics and Data Acquisition . . . . .	24
4.3	Basic Silicon Pixel Technology . . . . .	24
4.3.1	Detector Substrate . . . . .	24
4.3.2	Readout Chip . . . . .	25
4.3.3	Bump Bonding . . . . .	26
4.3.4	Detector Tiles . . . . .	26
4.4	General Detector Layout . . . . .	26
4.4.1	Detector Planes . . . . .	26
4.4.2	Mechanical Integration . . . . .	29
4.4.3	Electronic Integration . . . . .	29
<b>5</b>	<b>Test Set Up for 1996</b>	<b>31</b>
<b>6</b>	<b>Time Schedule, Responsibilities and Cost</b>	<b>32</b>
6.1	Time Planning for the Horizontal FPS Stations . . . . .	32
6.2	Time Planning for the Installation of Si-Pixel Detectors . . . . .	32
6.3	Responsibilities for the Si-Pixel Upgrade . . . . .	32
6.4	Cost Estimate for Horizontal Stations . . . . .	33
6.5	Cost Estimate for the Si-Pixel Upgrade . . . . .	33
<b>7</b>	<b>Summary</b>	<b>33</b>
<b>A</b>	<b>Comparison with ZEUS</b>	<b>36</b>
<b>B</b>	<b>Russian Micro-Channel-Plate Photomultiplier</b>	<b>37</b>

# 1 Introduction

Diffractive processes in deep inelastic electron–proton scattering and photo-production reactions are seen at HERA at a rate of about 10 % of the observable cross section. An investigation into these processes will open a new window to the understanding of diffractive phenomena well known in hadronic reactions. They are characterized by energetic protons at very small scattering angles, which in general leave the main detectors through the beam pipe. During the running period 1995 H1 operated a forward proton spectrometer (FPS) consisting of two detector stations 81 and 90 m downstream the interaction point in which scintillating fiber hodoscopes were approaching the circulating proton beam from above. A perspective view of the detectors, which reside in plunger vessels, is sketched in Figure 1.

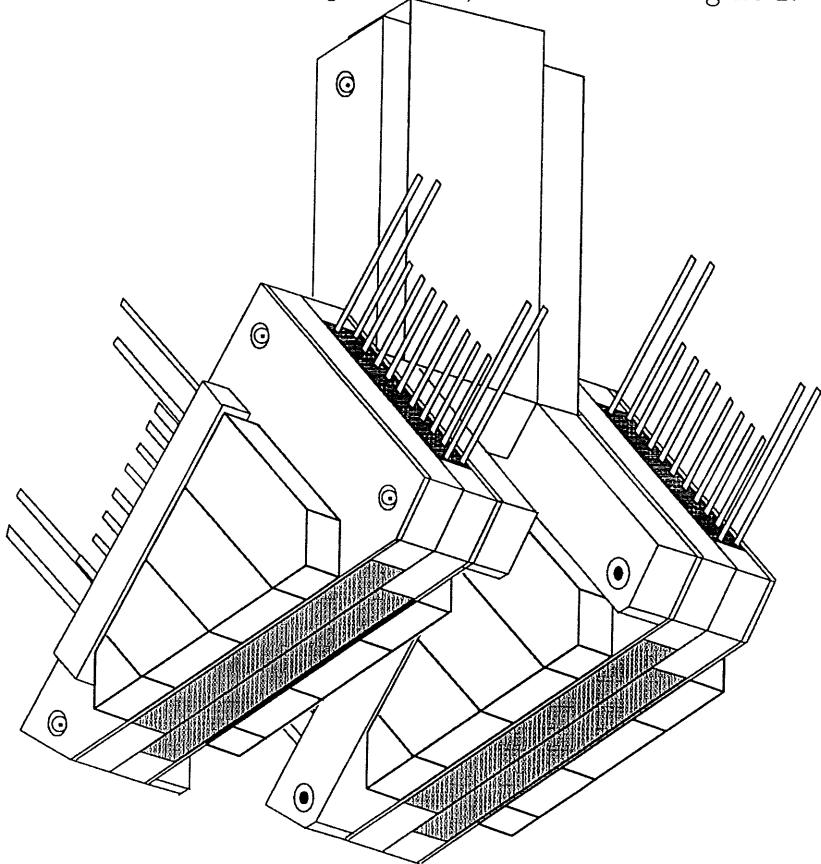


Figure 1: Perspective view of trigger tiles and scintillating fiber hodoscopes of a detector unit inside a Roman Pot.

The so called Roman pots were fully instrumented during the shut down 1994/1995. The layout of the system is described in the technical proposal PRC 94/03 and the experience gained during the 1995 running period proved the validity of the design principle showing that all components behaved according to their specifications. A total luminosity of about  $3 \text{ pb}^{-1}$  was accumulated, which will enable a physics analysis in terms of diffractive photo-production reactions with real and virtual photons.

The two existing FPS stations should be considered as a first step towards a more complete spectrometer with additional detectors at different distances from the interaction point in order to cover the whole kinematic range of proton momenta. The two vertical stations at 81 and 90 m cover the the high end of the pomeron spectrum with  $x_{IP} \geq 0.02$ , where  $x_{IP}$  is the fractional

Observed rates	
Single tile rate 81 m	50 kHz
Single tile rate 90 m	20 kHz
single pot trigger rate	5 kHz
81 m * 90 m	1 kHz
fps && etag && dcrphi	0.4 Hz
fps && zvtx_t0	20 Hz

Table 1: Observed Rates in H1 luminosity runs. The following abbreviations are used: fps: coincidence between both stations, etag: electron detected in small angle electron tagger, dcrphi: track from vertex in central jet chamber, zvtx\_t0: track pointing to main vertex in  $z$ .

momentum carried by the interacting pomeron in a diffractive process. This proposal describes an upgrade of the H1 forward proton spectrometer to access also lower values of  $x_{IP}$  down to  $10^{-5}$ . Two measures will be taken to achieve this goal. It is proposed to add two new stations at 63 and 80 m, in which the circulating beam will be approached in the bending plane of the machine (sideways) and to add high resolution Si-pixel detectors to the standard scintillating fiber detectors.

## 2 Performance of the FPS During the 1995 Running Period

Moving the plunger vessels close to the circulating proton beam does not create any problem if the approach is controlled by a set of counting rates, which are sensitive to protons interacting with the material of the plunger vessels and to particles passing both stations.

In typical luminosity runs about 55 mA proton currents were colliding with 30 mA electron beams. For these conditions with the Roman pots a few millimeters away from the circulating proton beam, the single rates recorded in the largest trigger tiles at 81 and 90 m were of the order of 50 kHz. Initial problems with synchrotron radiation hitting the detectors at 81 m, were solved by adding an appropriate lead shield. The coincidence rate for three out of four trigger planes in each station is of the order of 5 kHz. The coincidence rate between the two stations is about 1 kHz. The observed rates were acceptable also, when the HERA-B target was moved into the halo of the proton beam and allowed smooth operation of the FPS. Average counting rates measured in standard luminosity runs are summarized in Table 2.

The efficiencies of the trigger tiles for a typical luminosity run are displayed in Fig. 2. In this figure particularly low efficiencies are observed for the small trigger tiles at the edge of the hodoscope. By changing the light guides of all trigger tiles during the winter shut down 1995/1996 the efficiencies will be improved to well above 95%.

The efficiencies of the scintillating fiber hodoscopes are inferred from reconstructed tracks. Efficiencies of single fiber layers of 60% up to 70% can be read off Fig. 3. These numbers agree well with data obtained in test beam runs and Monte Carlo simulations of the fiber hodoscopes.

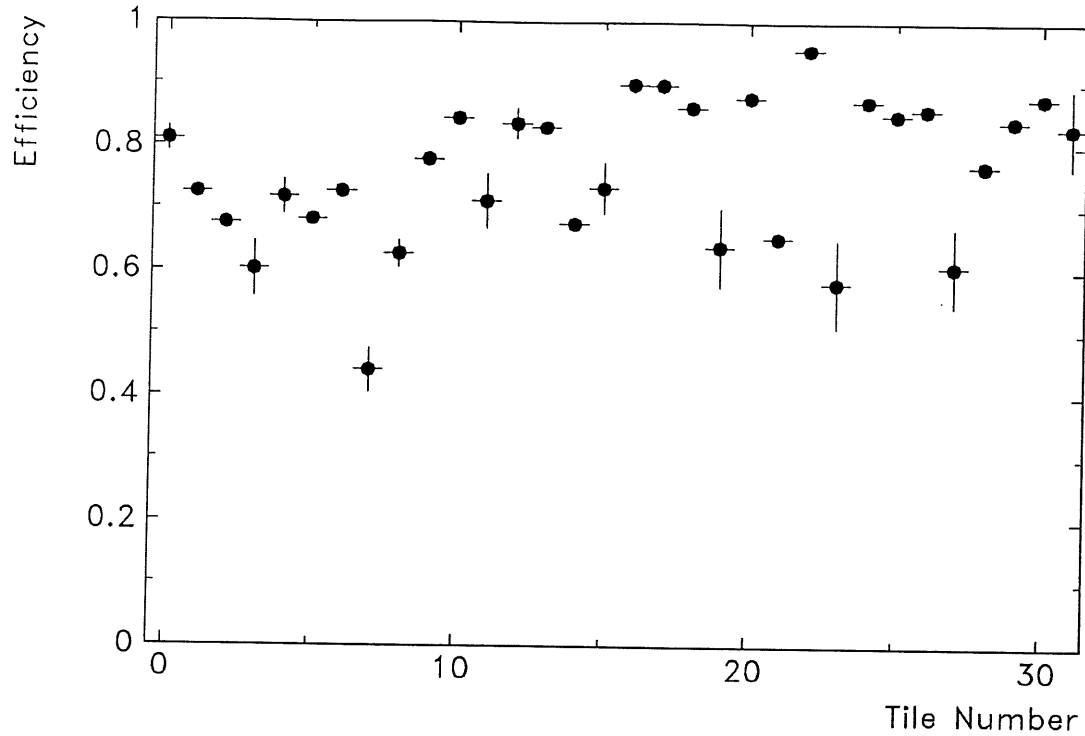


Figure 2: Efficiency of the 32 trigger tiles. Tiles 0 – 15 belong to the 81 m station, tiles 16 – 31 are in the 90 m station.

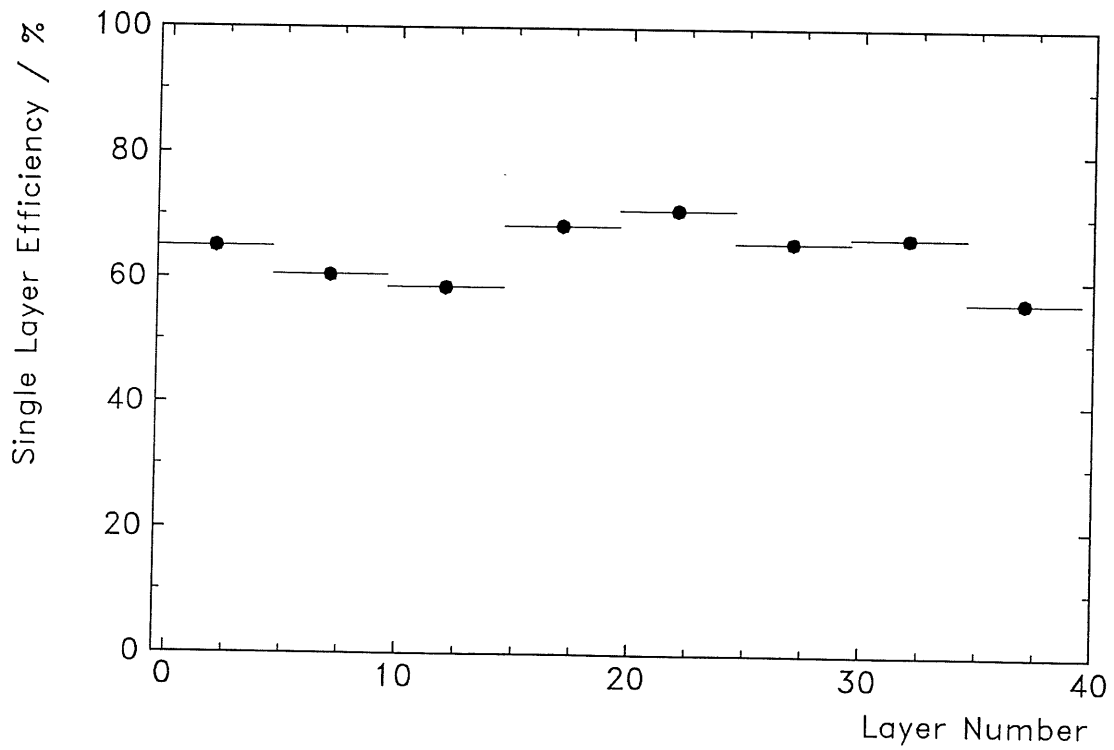


Figure 3: Single Layer Efficiency of the 8 Sub-detectors. Channel numbers 0 – 19 belong to the 81 m station, channels 20 – 39 to 90 m.

As there are ten layers per coordinate in each station from which at least five are requested to fire on a reconstructed track, one obtains a reconstruction efficiency between 80 and 90% for one coordinate.

The reconstruction of proton momenta requires the knowledge of the vertical position of the proton beam with respect to the nominal beam orbit. The beam position is monitored by the interaction vertex reconstructed inside the H1 detector and four monitors at various distances from the collision point, which are updated every two minutes. The beam stability over a typical luminosity run is of the order of 1/2 millimeter as demonstrated in the plots of Fig. 4 for the vertical beam position. A similar plot can be shown for the horizontal beam position monitors.

The values of the geometrical constants, which enter into the reconstruction of momenta, will be determined in a re-survey of the Roman pots and the precision beam position monitor in the HERA tunnel after the end of the 1995 running period. Thus at present the absolute energy calibration of the FPS is not very well known and the measured momenta are subject to a common offset.

The momentum determination for protons starting at the interaction point relies on the fact that the two measurements of the longitudinal momentum  $p$  by making use of the dispersion in the horizontal ( $p(x)$ ) and vertical ( $p(y)$ ) planes have to agree with each other within errors. This method is described in detail in the technical proposal PRC 94/03. Fig. 5 shows the correlation between the two measurements without geometrical corrections, assuming design values for all geometrical constants. In this plot the momenta around 820 GeV are unphysical. They originate from imperfections in the present set of calibration constants and protons which do not have their origin at the interaction point. Otherwise a clear correlation is visible with a width of about 1.8% in Fig. 5 b. Also shown in this figure is the type of improvement that can be expected after corrections to the geometry. A first guess for the position of the interaction point in H1 and the beam positions at 81 and 90 m improves the correlation between the x and y measurements of the scattered protons as shown in Fig. 5 c and the momentum resolution in Fig. 5 d. Work on the momentum reconstruction has just started but already now there are indications that a resolution well below 1% can be achieved.

Like the momentum reconstruction also the determination of the proton scattering angle at the interaction point, which is shown in Fig. 6, is subject to uncertainties in the calibration constants. In Fig. 6 some unphysical angles are observed around and above 2 mrad. These events are most likely due to proton beam gas interactions.

In order to demonstrate the capability of the FPS trigger an event is shown in Fig. 7, which is a candidate for diffractive photo-production with a proton seen in the two stations at 81 and 90 m.

Summarizing the experience that was gained during the 1995 luminosity runs on the operation of the FPS with two stations at 81 and 90 m, it can be stated that this component of H1 worked very reliably and the goals specified in the technical proposal PRC 94/03 were reached. The detectors and the read out system turned out to be very robust against varying beam conditions and data taking was continued also during periods, when the wire target for HERA-B was moved into the fringe of the proton beam.

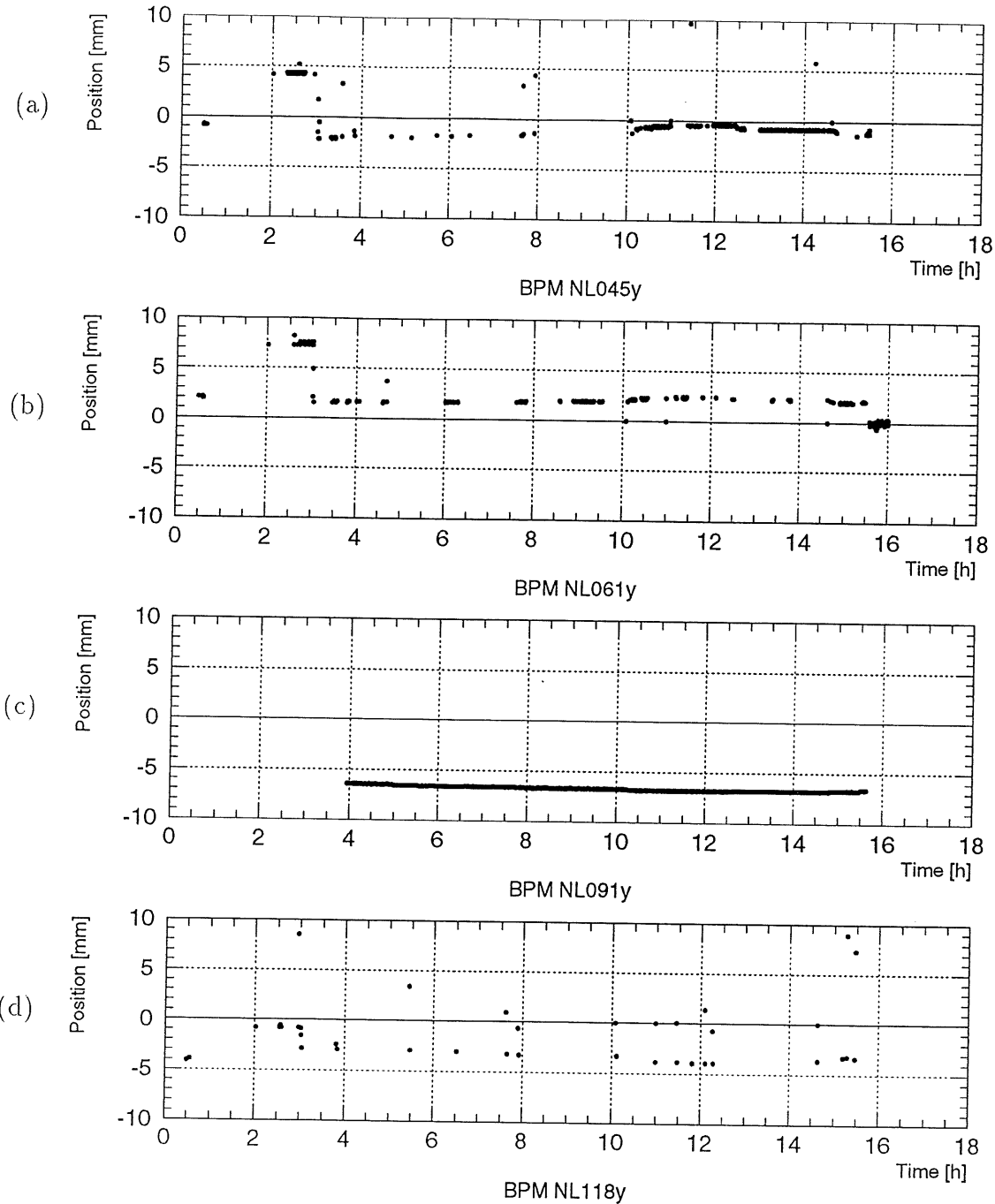


Figure 4: The y-position of the proton beam versus time during the fill 970 on October 25 1995, as measured by the HERA beam position monitors at 45 m (a), 61 m (b) and 148 m (d) and by the FPS device at 91 m (c) in the octant North left of the HERA proton ring. Fluctuations of more than 1 mm indicate read out and measurement instabilities.

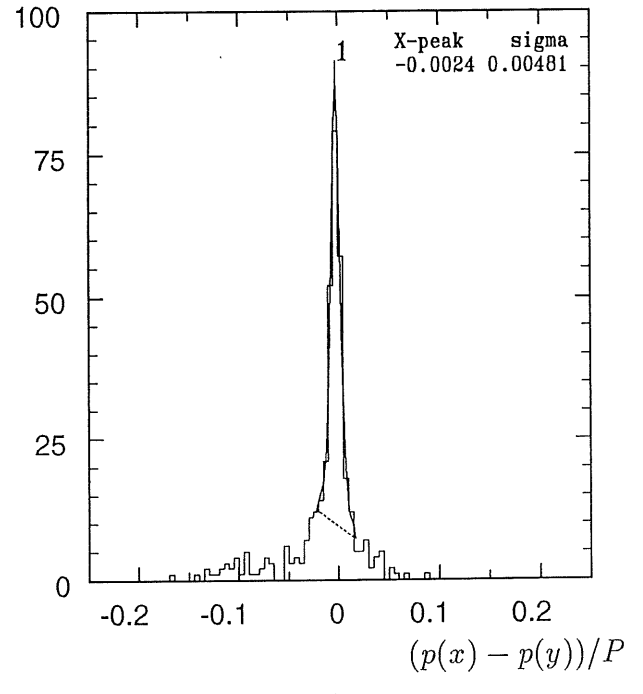
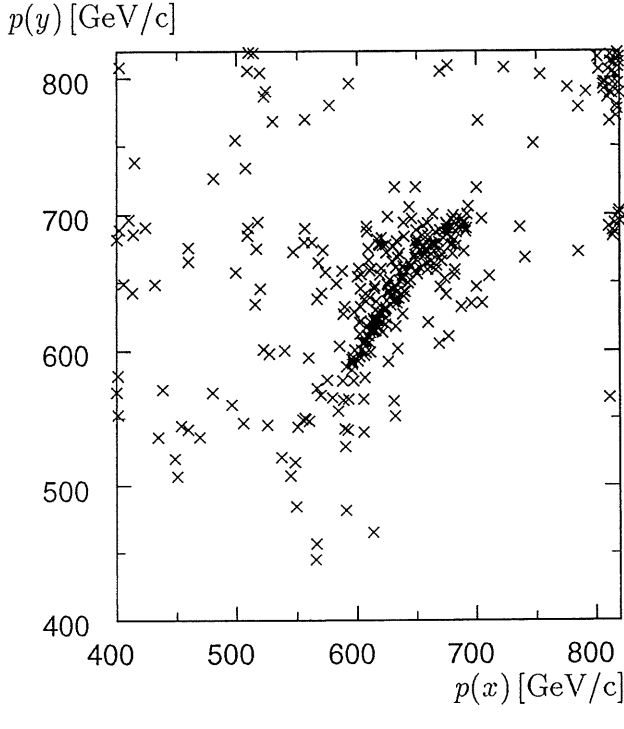
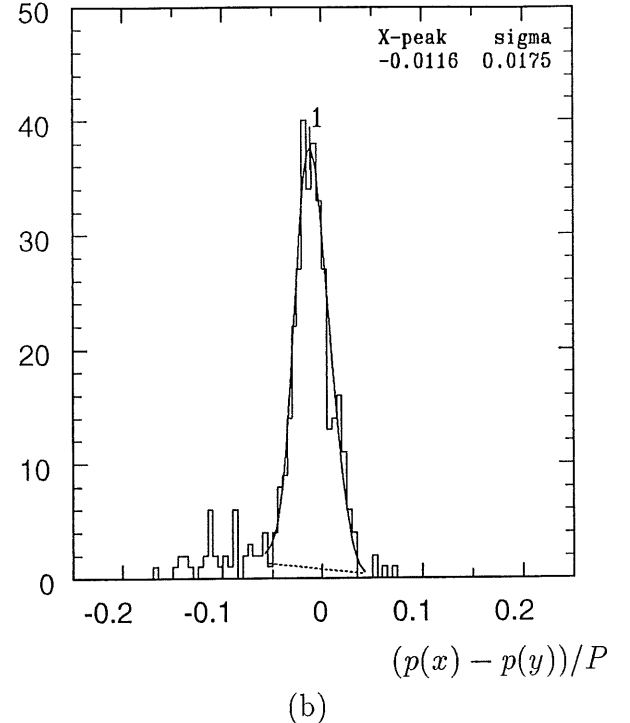
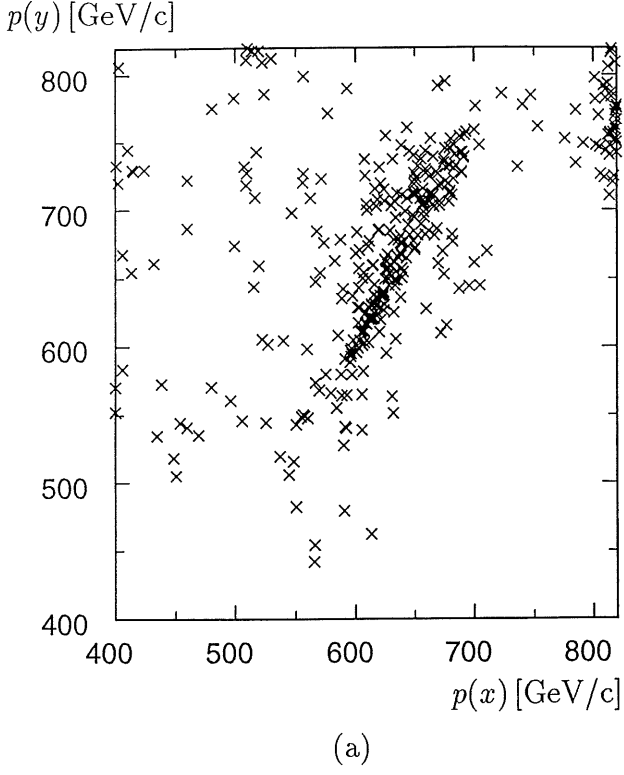


Figure 5: Figure (a) shows the correlation of the reconstructed momentum in the horizontal,  $p(x)$ , and the vertical plane,  $p(y)$ , the momentum resolution in figure (b). No corrections were done for the detector positions relative to the proton reference orbit. For (c) and (d) the distance to the reference orbit was decreased by 7 mm and the vertex position was shifted in the vertical direction by +3 mm (H1 run–vertex).

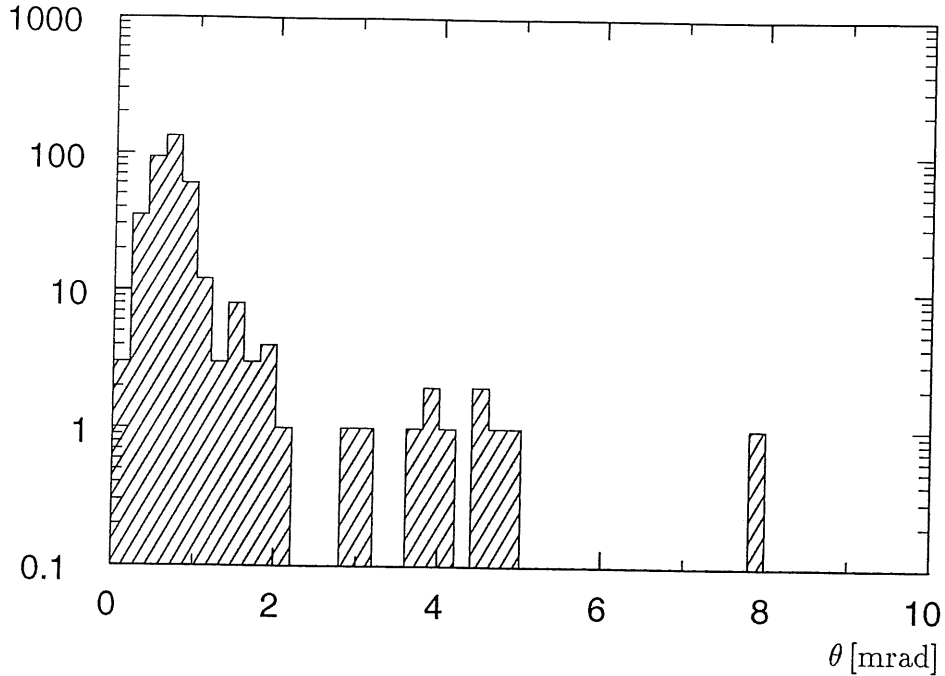


Figure 6: Proton scattering angle at the interaction point reconstructed assuming nominal geometrical constants.

### 3 The Physics Case for an Upgrade of the FPS

It was pointed out in the technical proposal PRC 94/03 that the two stations at 81 and 90 m cover only the kinematic range of large values of the fractional momentum carried by the interacting Pomeron  $x_{IP} \geq 0.02$  or equivalently the regime of large masses diffractively produced. The H1 collaboration was aware of the limited acceptance of the present set up and had already in the proposal stage announced further upgrades of the FPS which would extend the accessible  $x_{IP}$  interval to lower values of this variable. To reach this goal protons have to be detected, which carry essentially the full momentum of 820 GeV.

Two extensions of the present set up are proposed with the aim to improve the physics potential of the FPS. The H1 collaboration intends to add two additional stations 63 m and 80 m behind the interaction point, with which the circulating proton beam will be approached sideways in the horizontal plane and to add high resolution Si-pixel detectors to the existing scintillating fiber hodoscopes.

#### 3.1 Horizontal Stations at 63 and 80 m

To study the physics impact of detector stations at 63 and 80 m, which will record scattered protons by a coincidence measurement between the two, the distribution of diffractively scattered protons in a plane perpendicular to the beam at 63 m and 80 m is plotted in Fig. 8. There those protons are marked with stars, which are detected by a coincidence measurement, if the detectors are placed  $10 \sigma$  away from the center of the stored proton beam. According to the experience of the ZEUS collaboration, who operate a similar Roman pot device at the

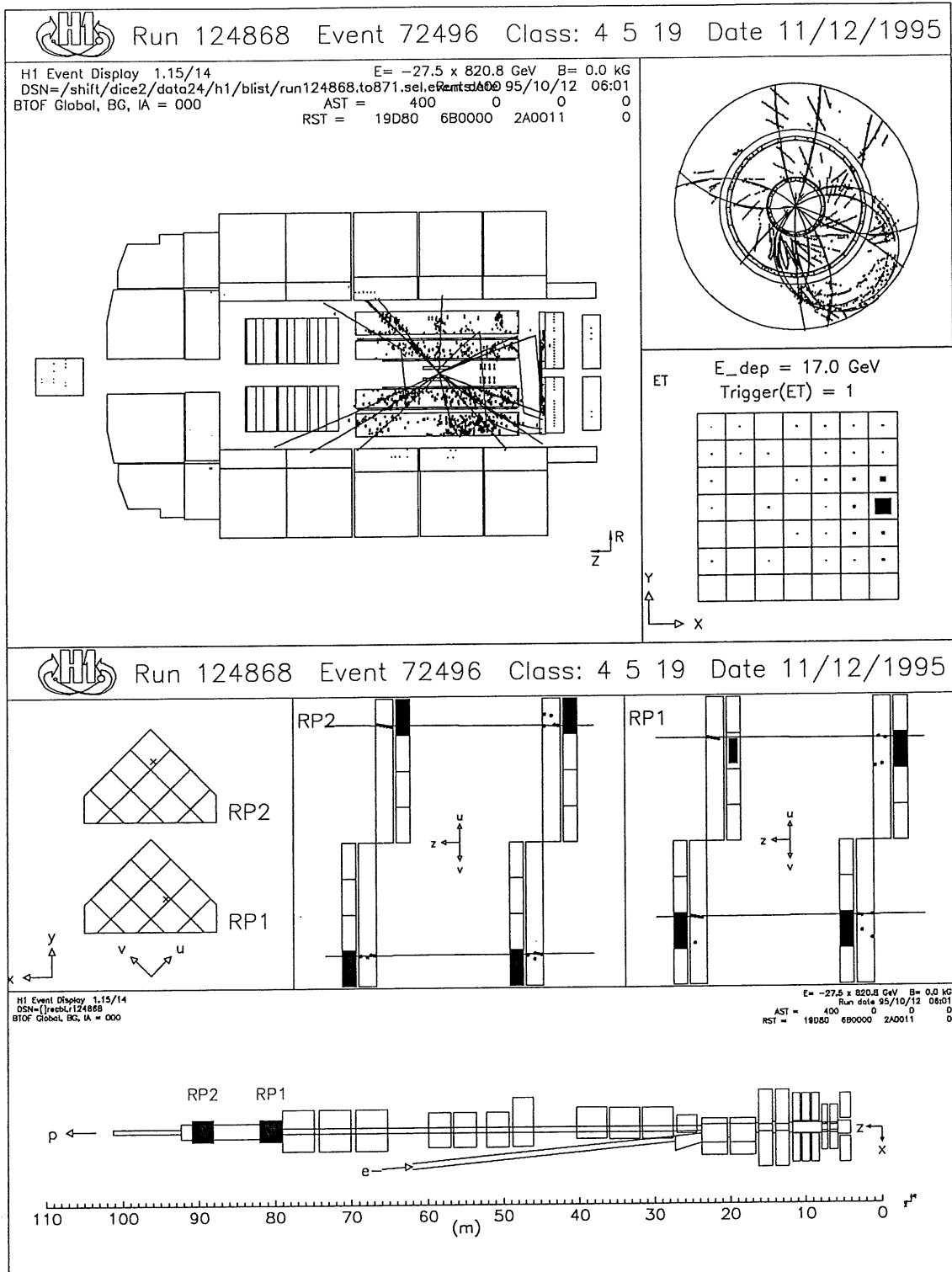


Figure 7: Tagged photo-production event with a track seen in both pots (upper half of lower figure) and some activity in the central detector.

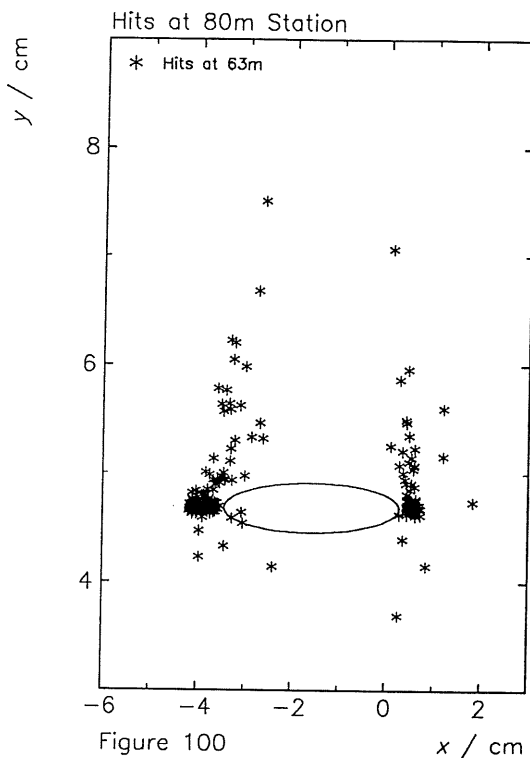


Figure 100

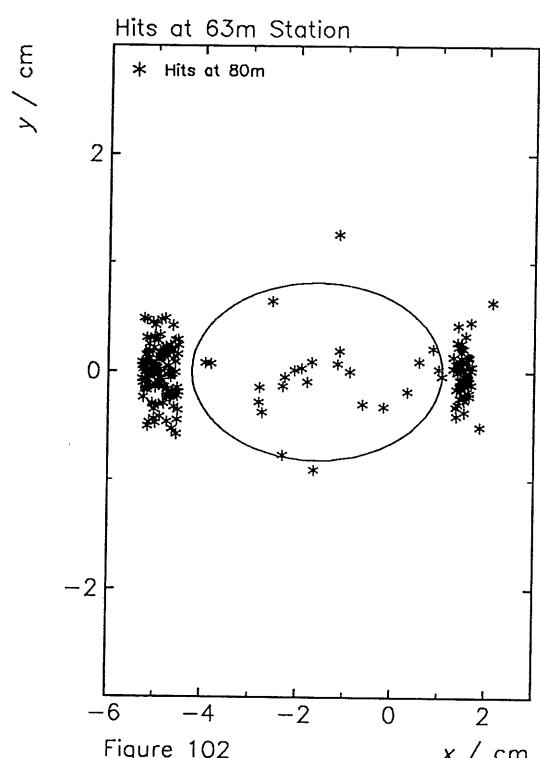


Figure 102

Figure 8: Hit positions at 63 m for protons from diffractive processes crossing a plane perpendicular to the beam at 80 m outside  $10\sigma$  (left picture) and hit positions at 80 m for protons crossing a plane perpendicular to the beam at 63 m outside  $10\sigma$  (right picture). The ellipses shown represent the  $10\sigma$  beam profiles.

same positions in the HERA machine, an approach to within  $10\sigma$  of the beam envelope is possible still finding reasonable background conditions. Under these conditions about 5% of all diffractive events will be recorded with a fully reconstructed scattered proton.

To demonstrate the improvement in acceptance for diffractive processes, Figure 9 compares the range in the variable  $x_{IP}$ , accessible to H1 for the present set up with an upgrade by two additional horizontal pots at 63 and 80 m. While the present set up covers large values of  $x_{IP} \geq 0.02$  the addition of two horizontal stations extends the acceptance range down to  $x_{IP} = 10^{-5}$ . Lowering  $x_{IP}$  is equivalent to an extension of the acceptance to lower masses of the diffractively produced hadronic final state  $M_X$  down to the masses of elastically produced vector mesons as demonstrated in Fig. 10.

The over all acceptance of the additional stations at 63 and 80 m with horizontal pots is of the order of 5% of the diffractive cross section. Acceptances in terms of the kinematic variables  $x_{IP}$  and  $M_X$  are compared in figures 11 and 12 with the upgraded version of the FPS. The acceptances were determined from an event sample in a kinematic range, where the electron can be detected in the small angle electron tagger which has an acceptance of about 30%. On top additional triggers in the central detector may fire. The small fraction of events, for which a forward going proton will be recorded, is compensated by the fact that the cross sections at small  $x_{IP}$  and small masses  $M_X$  are large of the order of 20  $\mu\text{barn}$ .

### 3.1.1 Resolution

In order to estimate the resolution, which can be expected by installing detectors at 63 and 80 m, lines of constant energy and emission angle are plotted for the 63 m position in Figures 13 a and b. These plots show the sensitivity of momentum - and scattering angle measurements with respect to the spatial - and angular resolution with which trajectories can be determined by the Roman pot devices.

Table 3.1.1 summarizes all significant errors, which will limit the resolution of the FPS. The momentum measurement is based on a determination of the slope of the trajectory between 63 and 80 m, which is only affected by the spatial resolution, the alignment error and the multiple scattering error but not by the vertex smearing, because to first order the trajectories are displaced by the same amount at both positions. For a detector resolution of 100  $\mu\text{m}$ , which is typical for scintillating fiber hodoscopes, all three contributions to the momentum resolution are of about the same size. The resolutions quoted in Table 3.1.1 assume a vertex resolution of 55  $\mu\text{m}$ , which will be achieved with the central Silicon tracker of H1. detector of H1. Thus in case the detector stations at 63 and 80 m are equipped with scintillating fiber hodoscopes the energy of diffractively scattered protons will be measured with an uncertainty of 5 GeV and an angular resolution of 2  $\mu\text{rad}$ . However, reconstructing the transverse momentum, the divergence of the proton beam at the interaction point has to be taken into account. Therefore an additional uncertainty of 30  $\mu\text{rad}$  has to be considered, which dominates the resolution resulting in an uncertainty of 25 MeV, a number adequate for investigating diffractive cross sections as a function of the momentum transferred to the proton.

## 3.2 Upgrade with Si–Pixel Detectors

Although the range in  $x_{IP}$  between  $10^{-5}$  and 0.3 is covered by the proposed set up with two vertical and two horizontal stations, the overlap in the range of kinematic variables between them

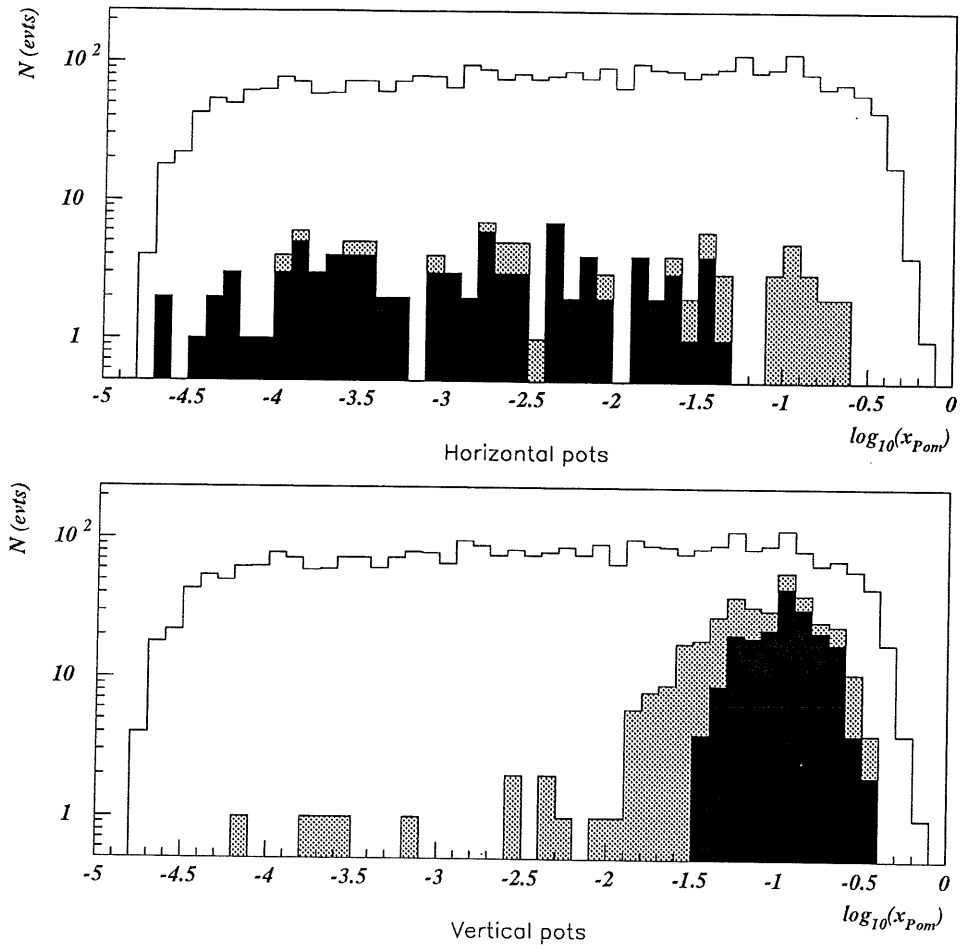


Figure 9: Acceptance of the horizontal and vertical pots, with detectors positioned at  $1.7\text{mm} + 10\sigma$  from the beam. The black area corresponds to protons detected in coincidence between the two pots of the sub-system, and the grey area to those crossing the 63 m (respectively 90 m) detectors alone. The white histogram corresponds to the total generated sample.

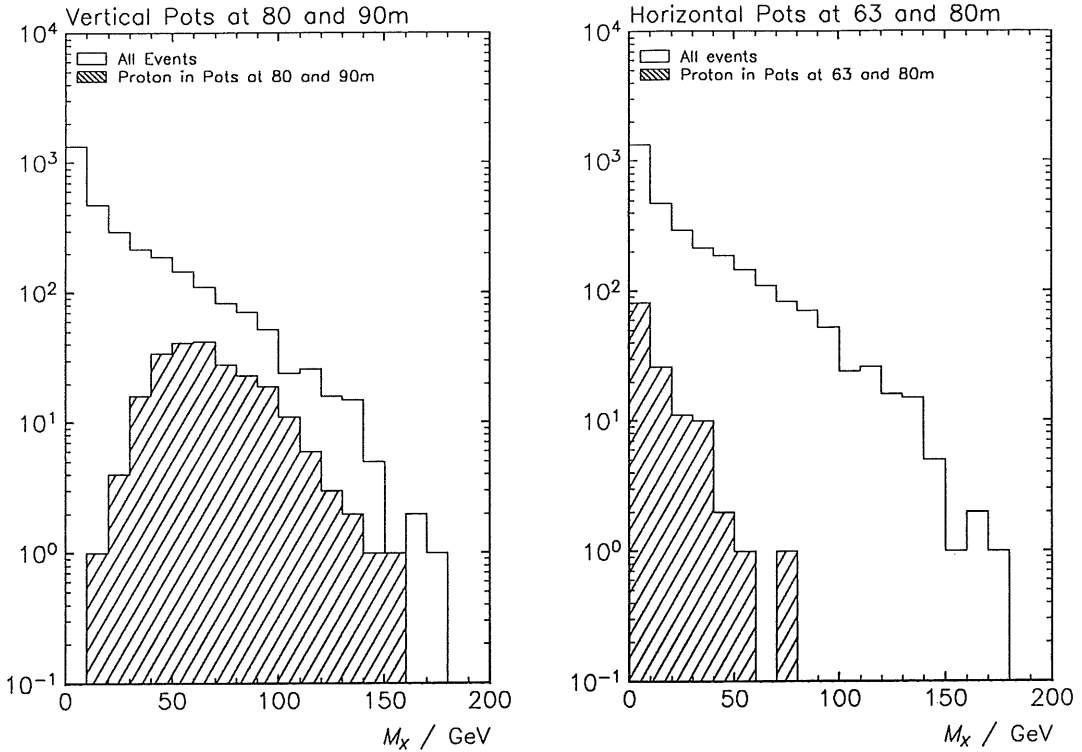


Figure 10: Distribution of the mass  $M_X$  of the hadronic final state (without the scattered proton) for diffractive processes. The hatched area corresponds to events where the scattered proton is detected in the existing vertical pots at 81 and 90 m (left), or in horizontal pots at 63 and 80 m (right).

Spatial resolution x coordinate	$\sigma(x) = 100 \mu\text{m}$
Spatial resolution y coordinate	$\sigma(y) = 100 \mu\text{m}$
Alignment 63 m versus 80 m	$\sigma(x_{align}) = 100 \mu\text{m}$
Alignment 63 m versus 80 m	$\sigma(y_{align}) = 100 \mu\text{m}$
Multiple scattering	$\sigma(\theta) = 6 \cdot 10^{-3} \text{ mrad}$
Effect of vertex smearing on x coordinate	$\sigma(x) = 110 \mu\text{m}$
Effect of vertex smearing on y coordinate	$\sigma(y) = 100 \mu\text{m}$
Effect of vertex smearing on slope $dx/dz$	$\sigma(\theta_x) = 0.4 \cdot 10^{-3} \text{ mrad}$
Effect of vertex smearing on slope $dy/dz$	$\sigma(\theta_y) = 1.1 \cdot 10^{-3} \text{ mrad}$
Beam divergence at the IP	$\sigma(\theta_x) = 30 \cdot 10^{-3} \text{ mrad}$
Beam divergence at the IP	$\sigma(\theta_y) = 90 \cdot 10^{-3} \text{ mrad}$
Energy resolution	$\sigma(E) = 5 \text{ GeV}$
Scattering angle (intrinsic)	$\sigma(\theta_{scatt}) = 2 \cdot 10^{-3} \text{ mrad}$
Transverse momentum (incl. beam spread)	$\sigma(p_t) = 25 \text{ MeV}$

Table 2: Resolution.

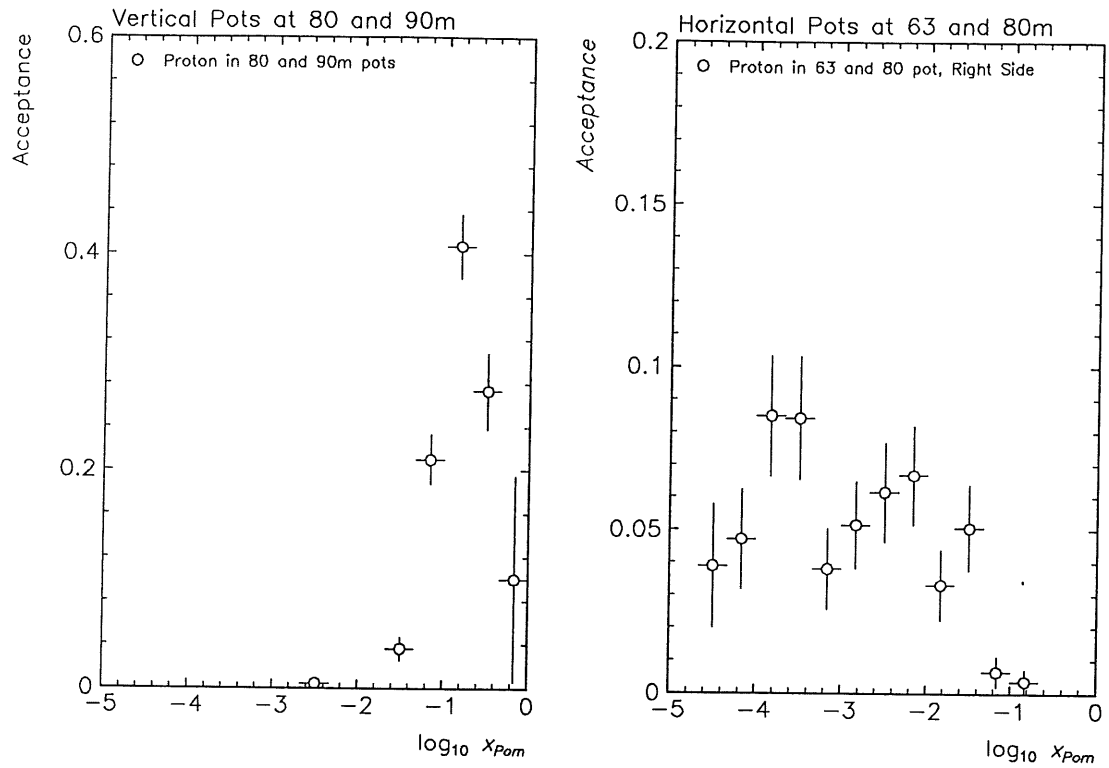


Figure 11: Acceptance of the existing vertical pots at 81 and 90 m (left) and the proposed horizontal pots at 63 and 80 m (right) as a function of  $\log_{10} x_{IP}$ .

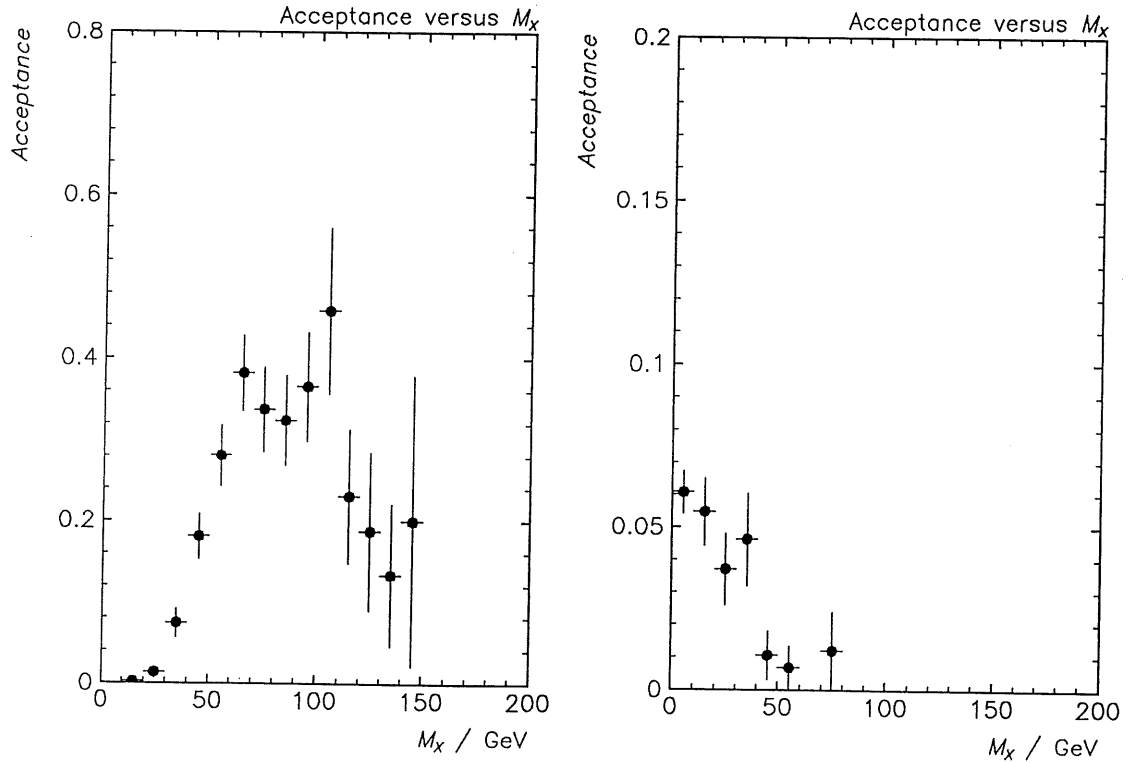
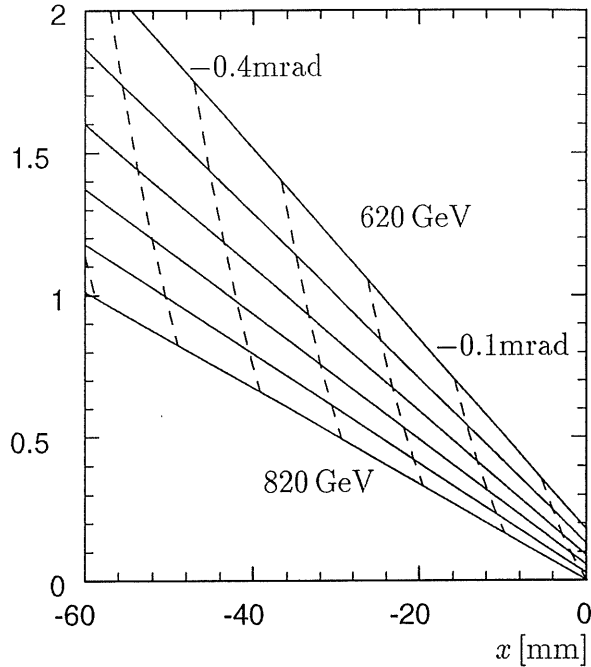


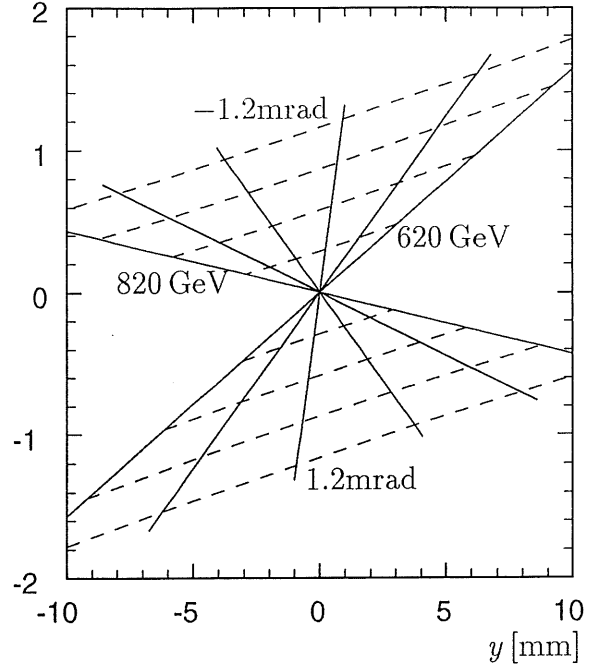
Figure 12: Acceptance of the existing vertical pots at 81 and 90 m (left) and horizontal pots at 63 and 80 m (right) as a function of  $M_x$ .

$dx/dz$  [mrad]



(a)

$dy/dz$  [mrad]



(b)

Figure 13: Lines of constant energy and scattering angle as a function of the a) horizontal coordinate  $x$  and b) vertical coordinate  $y$  versus the corresponding slopes of the trajectories at 63 m.

is uncomfortably small for cross checks and cross calibration. Therefore a larger acceptance of the vertical spectrometer part would improve the physics capability of the FPS considerably. This goal can be reached by adding high resolution Si-pixel detectors to the fiber hodoscopes. At the same time the momentum resolution of the FPS will be improved.

### 3.2.1 Intrinsic Pixel Detector Resolution and Efficiencies

Roman pots equipped with 2 detector planes made of  $50 \times 360 \mu\text{m}^2$  pixels will provide a spatial resolution of  $10 \mu\text{m}$  in the radial direction and  $52 \mu\text{m}$  in the azimuthal direction (see section 4.4.1). This has to be compared with the resolution of the present detector ( $100 \mu\text{m}$  in both directions) and the limitations due to relative alignment of the pots (between  $50 \mu\text{m}$  and  $100 \mu\text{m}$ , alignment errors for vertical stations are smaller than those for horizontal stations) and multiple scattering (equivalent to  $50 \mu\text{m}$  per pot for tracks in coincidence in two pots). In addition, the radial deflection angle can be measured in a single pot with a resolution of  $200 \mu\text{rad}$ , more than an order of magnitude better than that achieved with the present detectors ( $3 \text{ mrad}$  at nominal resolution). Finally, pixel detector planes have a detection efficiency close to 100 %.

The impact on diffractive physics of such an upgrade has been studied using a Monte-Carlo sample of diffractive events. Protons in the forward direction were simulated in the range  $300 < E_P < 820 \text{ GeV}$  and  $-1.1 < t < 0 \text{ GeV}^2$ , with a full description of the initial vertex smearing and beam optics. This beam line simulation is incorporated into the standard H1SIM Monte-Carlo program and has been cross-checked by comparing its results with the HERA beam

envelopes. The study reveals the main areas of potential gain for diffractive physics, depending on the choice of the pots to be instrumented, as discussed in the subsequent sections.

### 3.3 Impact of the 90 m Vertical Pot Instrumentation

As shown in figure 9, discarding the coincidence with the 81 m pot and measuring the trajectories with the 90 m pot only gains a factor 2 in acceptance of the vertical system. At a given distance from the beam (in terms of beam size sigmas) the 90 m pot catches more high energy protons than the 81 m pot (Fig. 14). This basic feature of the beam line is due to the fact that the 90 m pot is positioned at twice the distance from the vertical bending plane compared with the 81 m pot.

The energy of protons detected in the vertical system can be measured from a combination of the vertical impact and deflection only. As can be seen from figure 15, a resolution of  $200 \mu\text{rad}$  will allow to tag protons above 700 GeV with the 90 m pot alone.

This new single pot tagging possibility will double the global acceptance of the vertical system and extend it to the region  $10^{-2} < x_{P\bar{P}} < 10^{-1}$ . In this domain, the final hadronic state (excluding the proton) is still fully contained in the Liquid Argon Calorimeter, allowing an independent and more precise measurement of  $x_{P\bar{P}}$ . The enhanced region is of particular interest since it corresponds to the transition region between Pomeron (high proton energy) and meson (low proton energy) exchange dominance.

### 3.4 Impact of the Complete Instrumentation with Si–Pixels

Taking into account relative alignment and multiple scattering errors, the overall radial detector resolution will be improved from  $100 \mu\text{m}$  to  $50 \mu\text{m}$ . The proton energy measurement will be correspondingly improved at low energy (below 700 GeV), where it is known to be limited by the vertical deflection resolution. This is of interest for the determination of the neutral meson structure function, for which the initial meson energy cannot be reliably estimated from the central detector because the main hadronic system is not contained in the Liquid Argon Calorimeter.

In addition, the detector efficiency for proton tracks in coincidence between two pots will be considerably improved. Assuming a conservative efficiency of 97 % per pixel plane, more than 99 % of the protons will give at least 3 hits out of 4 in the 2 pots system, with both coordinates precisely measured.

## 4 Technical Description of the Upgraded FPS

The technical solutions to be employed in the FPS upgrade are based on the well proven technique of scintillating fiber hodoscopes for the new horizontal stations and on Si-pixel detectors to be attached to the fiber hodoscopes.

### 4.1 Fiber Detector

The principle and design of the detectors to be mounted into the horizontal plunger vessels is similar to the ones in the vertical stations. It is shown in Fig. 16. The fiber detectors are scaled to the appropriate dimensions and the design concept of the detector mechanics has

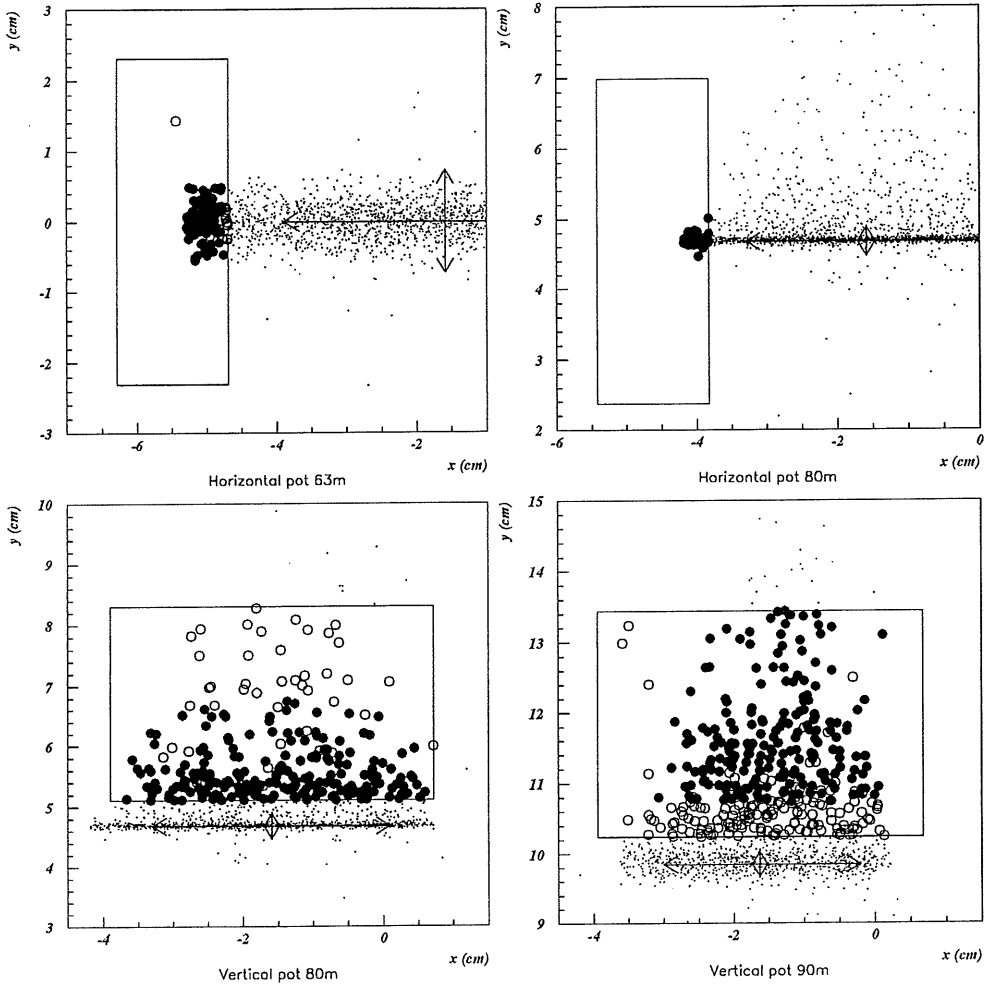


Figure 14: Hit positions of the protons crossing a plane perpendicular to the beam at 63 m, 81 m and 90 m. The rectangular boxes show the proposed pixel detector geometries for the 4 Roman pots. Open circles show protons detected in only one of the two pots of each sub-system (horizontal or vertical), whereas full circles show protons which are detected in both pots of the sub-system.

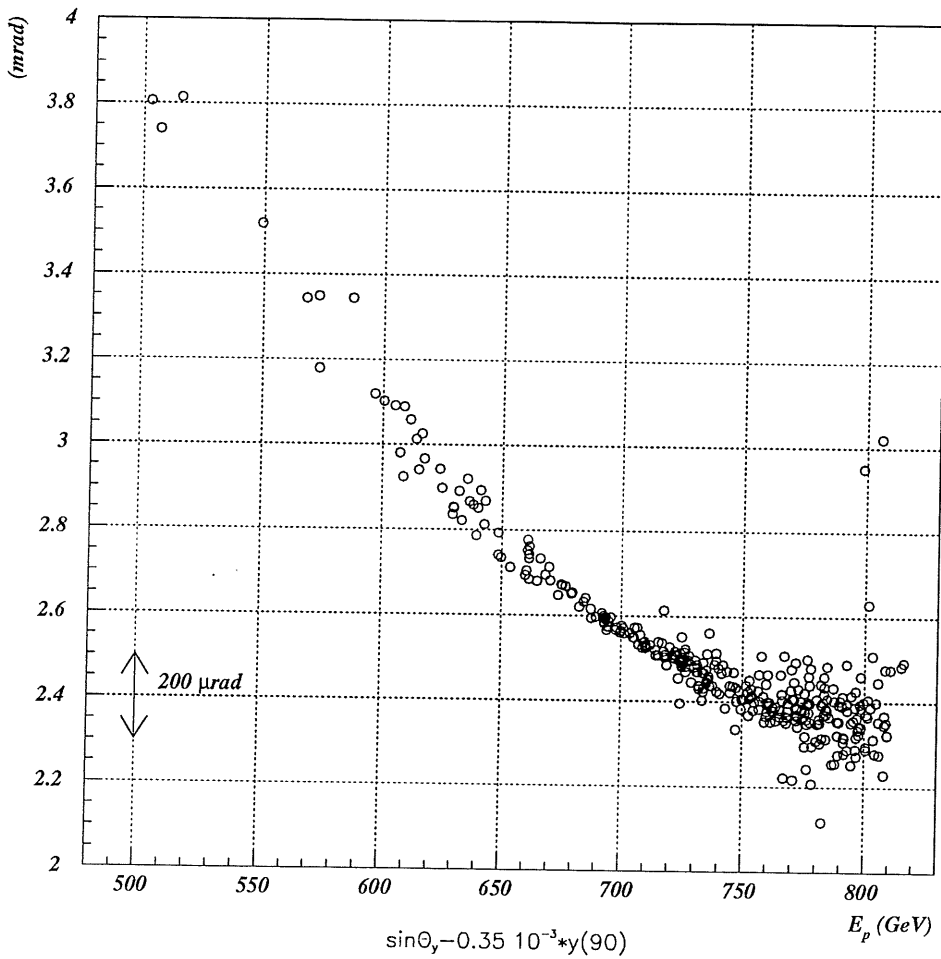


Figure 15: Plot of an energy tagging variable versus the proton energy. This tagging variable combines the proton deflection angle in the vertical direction and its vertical impact measured in the 90 m Roman pot. Using pixel detectors, a resolution of  $200 \mu\text{rad}$  (shown as an arrow on the plot) will be achieved on such a variable, which will allow to tag the high energy protons with the 90 m pot alone.

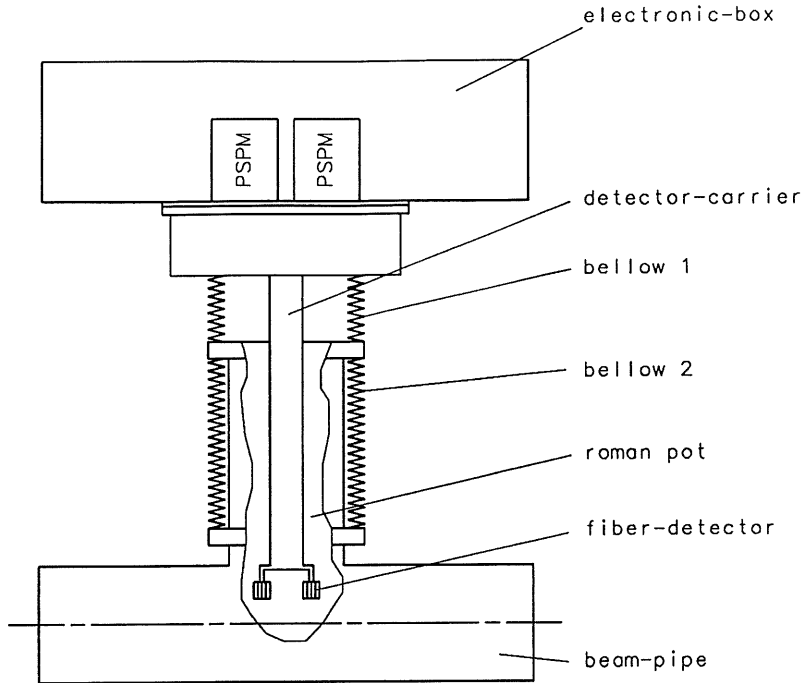


Figure 16: Scheme of the detector arrangement (top view) including beam pipe, fiber detector, PSPM's and electronic box.

to be matched to the restricted space between proton beam line and the tunnel wall or cable installation respectively.

Based on the 1995 experience during H1 luminosity runs there is no need to change the basic design of the fiber detectors. Therefore it is proposed to build a fiber detector consisting of two sub-detectors per station separated by about 60 mm which allow to suppress large angle background. The schematic of the arrangement of the fiber hodoscopes is shown in Fig. 17.

Each sub-detector consists of two coordinate fiber planes (u,v). Each coordinate detector consists of 5 layers of about 20 fibers of 1mm diameter (Fig. 18). The layers are staggered by  $210 \mu\text{m}$  (pitch/5). The sub-detectors are staggered to each other by  $105 \mu\text{m}$  (pitch/10). The scintillating fibers of the detector are thermally spliced to light guide fibers. The ends of the light guide fibers are glued into masks which match the pixel structure of the PSPMs. The mechanical support of the fiber detectors is similar to that used in the vertical pots. Adjacent to the fiber detectors the trigger planes are attached to a common support frame which also carries the Si-pixel detectors (Fig. 19).

#### 4.1.1 Optoelectronic Readout

The experience with the performance of the Hamamatsu PSPMs H4139-20 is quite good, so that the application of these tubes presents the smallest technical risk. Beside this, the quantum efficiency had been improved from tube to tube during the delivery period in 1995.

A group from JINR Dubna proposed the application of a PSPM based on Micro-Channel-Plates (MCP) with 100 pixels built in Moscow. This device was investigated in the laboratory and in test beams. An application to read out scintillating fiber hodoscopes in the FPS seems to

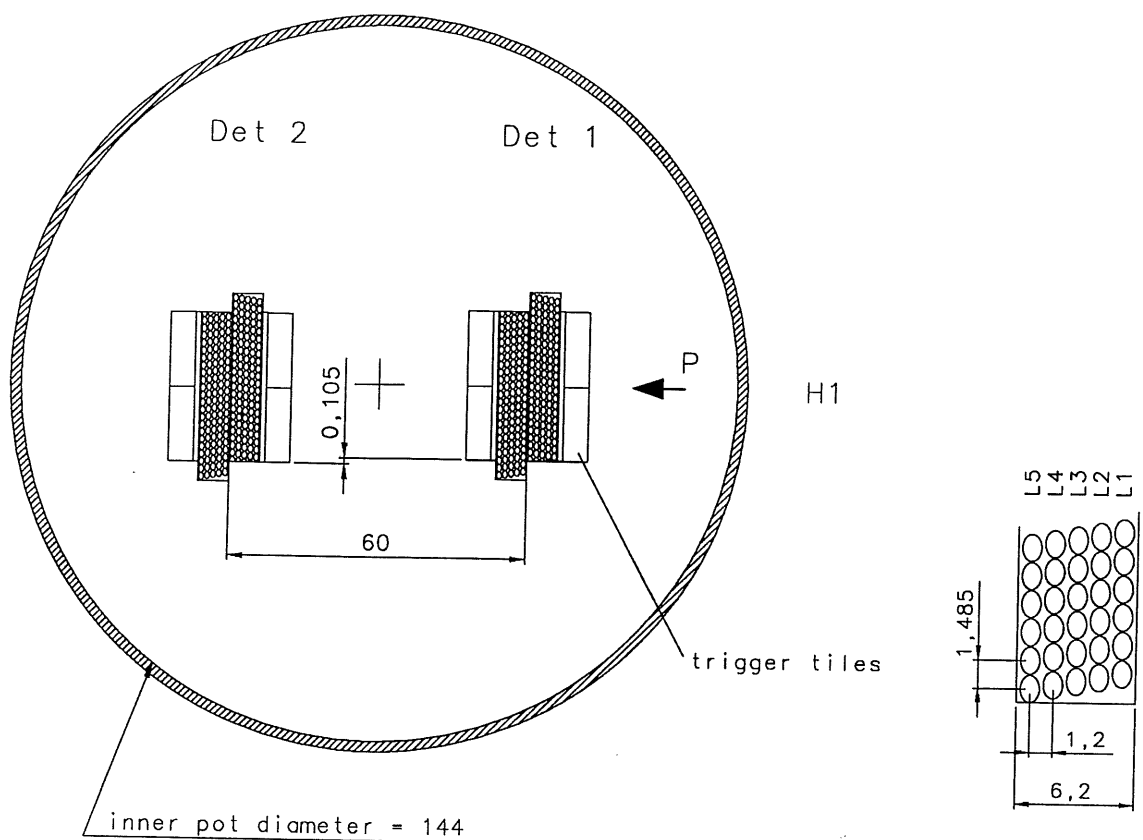


Figure 17: Arrangement of fiber planes (top view) consisting of two sub-detectors with trigger planes.

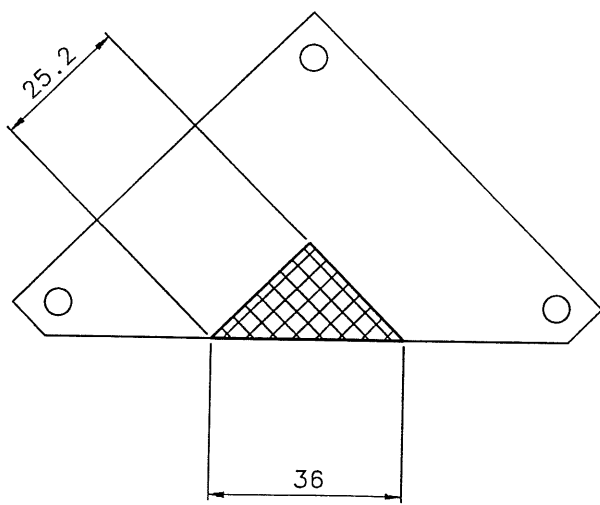


Figure 18: Fiber detector plane with 25 fibers per layer.

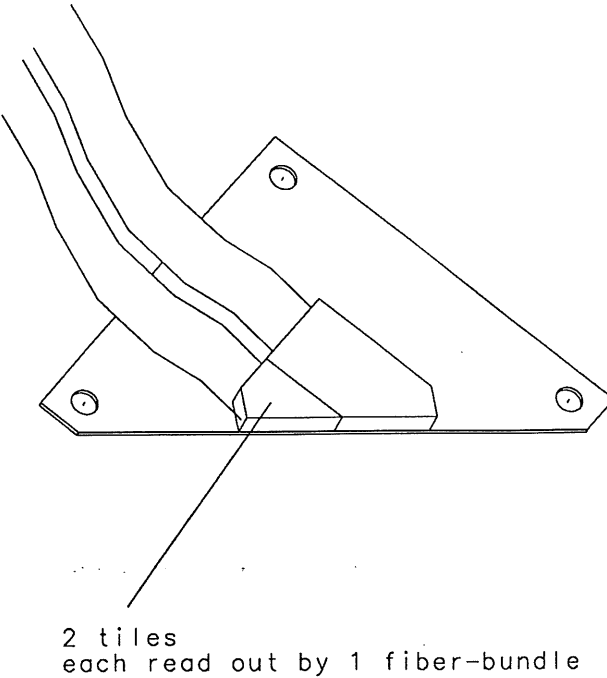


Figure 19: Trigger plane configuration for twofold multiplexing.

	H4139-20	MCP
No. of pixels	64	100
Pixel area	diam. 4mm	$1.5 \times 1.5 \text{ mm}^2$
Sensitive area	$40 \times 40 \text{ mm}^2$	diam. 25 mm
Quantum efficiency	20 %	$\geq 5 \%$
Gain	$10^6$	$< 3 \times 10^5$

Table 3: Comparison of basic data of the PSPMs

be possible. The main advantage of the device is its low price and good uniformity of response over the entire cathode surface. An improved version of Russian PSPMs will be available in January '96. In March '96 a final decision has to be made, which type of PSPM should be used. A description of the Russian PSPM and test results are given in Appendix A2.

The Moscow tube could be used without multiplexing whereas a twofold multiplexing is foreseen for the Hamamatsu option.

#### 4.1.2 The Trigger

The principle of the proposed trigger for the FPS is the same as that for the vertical stations. One plane of scintillator tiles per coordinate plane is foreseen, resulting in four planes per pot (2 subdetectors  $\times$  2 coordinates) as shown in Fig. 19.

The trigger planes serve two basic functions:

1. provide a first level trigger signal for charged particles traversing the station under small angles with respect to the beam line,
2. ambiguity resolution in the case of multiplexed optoelectronic readout of the fiber signals.

The light output of one scintillator tile, which is 5 mm thick, is collected by about 200 fibers with a diameter of 0.5 mm. They are read out by new small size PM R5600 (Hamamatsu), which are mounted inside the pot approximately 20 cm above the fiber-detector.

#### 4.1.3 Mechanical Precision

The precision with which a space point in one station has to be measured (about 100  $\mu\text{m}$ ), is demanding but it has been reached in the vertical stations of the present FPS. To obtain such an overall position error it is necessary to achieve a high manufacturing precision and a precise three dimensional alignment of the different components of the setup with respect to each other. So the position error of single fibers of the detector should not exceed 10  $\mu\text{m}$ . The errors for the arrangement of the fiber detector and the detector support should be of the order of some ten  $\mu\text{m}$ . The alignment error of the detector setup should not dominate the overall error for positioning the detector in the HERA coordinate system by surveying.

#### 4.1.4 Read–Out Electronics

The read-out electronics including front end cards and data transfer, which was used in the 1995 data runs proved to be adequate. Therefore it is proposed to duplicate the electronics and attach it to the horizontal FPS stations. In case the Russian version of PSPM's is used, a preamplifier has to be added, which is already available and which has been tested to match the input requirements of the standard electronics chain.

### 4.2 The HERA Si–Pixel Detectors

Silicon devices are sensitive to the exposure of ionizing radiation. Therefore the environment in which the pixel detectors will be operated has to be investigated prior to installation. It turns out that the environment and specifications for detectors close to the HERA beam pipe are similar to those encountered at the future LHC, but less severe in several respects.

#### 4.2.1 Radiation Levels

Ionizing radiations at the detectors positions originate from both the proton and the electron beams. Their order of magnitude can be estimated from several available measurements :

- for high energy radiation ( $> 30 \text{ keV}$ ), the values measured by H1 at the PLUG calorimeter position using thermo-luminescence dosimeters (about 30 krad per year, [1]) are compatible to those obtained in the same way by ZEUS at various positions along the beam pipe (100 krad in the worst case, [2]). Independent estimations using single hit counting rates in the H1 pots trigger scintillator tiles yield values of about 10 krad.
- low energy radiation ( $< 30 \text{ keV}$ , originating mainly from synchrotron radiation), is more difficult to measure because of the lack of sensitivity of thermo-luminescence dosimeters. From the damage observed at the surface of their silicon detector planes, the H1 PLUG group infers that values as high as 1 Mrad per year could be deposited by such low energy particles in the PLUG innermost channels [1]. Compared to the PLUG calorimeter, the H1 Roman pots are located further away from the electron beam by about 30 cm, and are shielded from it by a lead wall. The plunger vessel walls also provide a natural shielding of the detectors against low energy photons and electrons. Single hit rates in the pots

trigger tiles show that the lead wall reduces the synchrotron radiation hitting the pots by 2 orders of magnitude, and brings it back to a lower level than irradiation from the proton beam.

In summary, the level of ionizing radiation at the detector position is estimated between 10 and 100 krad per year, a factor 10 to 100 lower than that expected for LHC central trackers (about 2.5 Mrad/year, [3]).

#### 4.2.2 Electronics and Data Acquisition

In H1 the 10.4 MHz bunch crossing frequency requires from tracking detectors a time discrimination better than 96 ns, with signals pipelined during the 1st level trigger latency of about 25 bunch crossings. These requirements are similar to, but weaker than, those encountered in the future ATLAS experiment at LHC (40 MHz bunch crossing frequency and 80 BC's trigger latency, [3]). Another simplification compared to ATLAS is the 800  $\mu$ s first order dead time allowed for data readout, during which pipelines can stay frozen.

### 4.3 Basic Silicon Pixel Technology

The design of silicon pixel detectors for the H1 Roman pots is based on the expertise gained in building the DELPHI Very Forward Tracker [4] and in developing new detectors for the ATLAS experiment.

The DELPHI Very Forward Tracker (VFT, [4]) gathers 1500  $\text{cm}^2$  of detector made of  $330 \times 330 \mu\text{m}^2$  pixels, with an electronics implemented in standard non radiation hard technology. The detector is now in the assembly stage and will be installed at the beginning of 1996.

In the framework of the ATLAS central tracker developments, a first complete prototype of a  $8 \times 15 \mu\text{m}^2$  pixels detector, built by the CPPM in radiation hard technology with its full readout electronics, was beam-tested at CERN in summer 1995. Results [5] show that the H1 requirements are already essentially met by the LHC R&D.

#### 4.3.1 Detector Substrate

In contrast to what is planned for ATLAS, the less severe radiation environment encountered at HERA makes it possible to use the same detector thickness as for the DELPHI VFT. The detector will be made of 300  $\mu\text{m}$  thick n-type silicon with a p<sup>+</sup> implant segmented in rectangular cells (pixels). Such pixel detectors offer a signal of about 24000 electrons for minimum ionizing particles at normal incidence, to be compared to the typical electronic noise of 100 e<sup>-</sup> and a threshold spread of 400 e<sup>-</sup>. The expected detection efficiency is close to 100 %, operating the DELPHI VFT detectors with a threshold of 8000 e<sup>-</sup> yields a typical efficiency of 99 % per chip, with all chips above 95 %.

The high signal/noise ratio of pixel detectors makes them much more resistant to radiation than e.g. strip detectors.

The proposed pixel size is  $50 \times 360 \mu\text{m}^2$ . It is determined by the readout chip specifications and the present status of bump bonding technique.

#### 4.3.2 Readout Chip

Pixel signals are processed by readout chips directly bonded on the detector substrate and controlling an array of  $7.2 \times 8.0 \text{ mm}^2$  each (i.e. 20 columns of 160 pixels).

Three main readout schemes are currently being investigated for the ATLAS experiment. Out of them, the CPPM readout scheme includes an integrated signal pipelining and a full “on chip” 2-dimensional zero-suppression :

- pixels hit at a given BC encode their line number ( $1 \rightarrow 160$ ) into a columnar shift register, which will then move the datum to the periphery of the column by one step per BC. The column itself thus acts as a storage pipeline of the pixel data.
- when reaching the column periphery, each encoded pixel datum is stored into a columnar peripheral memory and starts an associated counter incremented by the BC clock. When the whole system is frozen by a L1 trigger, pixels hit at the corresponding BC can be identified by the fact that the sum of their “line number” and their associated counter is equal to the L1 trigger latency. Pixels obeying this relation are transferred from the peripheral memory into another memory directly accessible by the readout.
- in the case of H1, pipelines are frozen during the  $800 \mu\text{s}$  readout time. This gives the possibility to read the data from several BC’s around T0, by varying the L1 latency reference number when transferring the pixels from the peripheral memory into the readout memory.

The chips are built in the radiation hard process DMILL [6], being developed by the Commissariat à l’Energie Atomique (CEA/LETI) and which will be put on the market by Matra MHS in 1997. The DMILL target specifications include a radiation hardness to an irradiation of at least 10 Mrad. Prototype DMILL chips for LHC pixels detectors have shown a perfect behavior up to 5 Mrad and a small decrease of performance after an irradiation of up to 20 Mrad [7].

The basic specifications of the CPPM readout chip make it directly suitable for an H1 application. They were validated during summer 95 [5] when a prototype chip from the DMILL “HADRON” run bump-bonded to a pixel detector was tested on beam at CERN. Technical problems due to the process of this run were understood and solved for the DMILL “LEPTON” run which has been completed in October 95. This latest chip is under test and first results show a good behavior of both the analog and the digital parts.

The size of the pixel analog cell does not yet allow the building of  $50 \times 300 \mu\text{m}^2$  pixels with a 25 ns time discrimination as required for ATLAS, but the H1 specification (96 ns) can already be met with  $50 \times 360 \mu\text{m}^2$  pixels.

The first full readout chip for an array of  $14 \times 156$  pixels (13 columns of  $50 \times 480 \mu\text{m}^2$  pixels and 1 column of  $50 \times 360 \mu\text{m}^2$  pixels) has recently been sent to fabrication in the framework of the DMILL “MUON” engineering run. Compared to the beam test prototype, this chip provides the additional possibility to deactivate noisy pixels in order to reduce the average data yield. It also incorporates an auto-calibration feature for detailed threshold adjustment. The chip is expected to be back around March 96 and can serve as the basis for a Roman pot tile prototype.

### 4.3.3 Bump Bonding

The bump bonding consists in soldering the readout chips to the detector substrate establishing an individual contact between each pixel and its corresponding readout cell. Two processes presently provide the required spatial granularity of  $50 \mu\text{m}$ : the GEC-MARCONI process [8] and the LETI process [9]. For the H1 application, we propose to use the LETI process, which was successfully tested in the Summer 95 beam tests.

### 4.3.4 Detector Tiles

The small detector surface necessary for the H1 Roman pots can be covered using individual detector tiles of 6 readout chips only (Fig. 20). More conventional bussing techniques than planned for ATLAS can be used, in the same way as for the DELPHI VFT: control and data lines can be incorporated into the detector substrate, and power lines provided in Kapton circuitry.

## 4.4 General Detector Layout

### 4.4.1 Detector Planes

It is proposed to install two detector planes per Roman pot, with each plane made of 4 detector tiles for vertical pots and 2 detector tiles for horizontal pots. This will provide an active surface area of about  $43 \times 32 \text{ mm}^2$  for vertical pots and  $43 \times 16 \text{ mm}^2$  for horizontal ones.

From the experience with the ZEUS Leading Proton Spectrometer [2] and assuming an efficient deactivation of noisy pixels, operating the silicon detectors with a threshold of  $1/4 \text{ MIPS}$  will provide not more than a few additional hits to the genuine proton track impacts. The possible resulting ambiguities in reconstructing the proton track segment from two planes only can be easily resolved using the redundant information from the fiber detectors.

For a given plane (see figure 21), detector tiles will be fixed alternatively on each side of a common support made of ceramic and aluminum heat pipes, and overlap by a few pixel lines to avoid dead areas. The critical dead region on the edge of the plane close to the beam can be kept less than  $0.5 \text{ mm}$ . The whole detector plane will be surrounded by a Faraday cage made of a  $200 \mu\text{m}$  thick aluminized carbon foil. The total plane transverse size will be about  $8 \text{ mm}$  and corresponds to  $2.3 \%$  radiation length in average.

The spatial resolution per plane will be  $50/\sqrt{12} = 15 \mu\text{m}$  in the radial direction, and  $360/\sqrt{12} = 104 \mu\text{m}$  in the azimuthal direction (the nominal resolution of  $330/\sqrt{12} \mu\text{m}$  is reached by the DELPHI detectors). In order to improve the azimuthal resolution, the pixel detectors of the two planes can be staggered by half a pixel size ( $180 \mu\text{m}$ ). Combining the independent measurements from the two detector planes, the spatial resolution per pot will be  $15/\sqrt{2} = 10 \mu\text{m}$  in the radial direction and  $180/\sqrt{12} = 52 \mu\text{m}$  in the azimuthal direction taking advantage of the pixel staggering in this direction.

Assuming two planes distant by  $10 \text{ cm}$ , the pixel orientation provides the optimal angular resolution of  $200 \mu\text{rad}$  in the proton bending plane for both vertical and horizontal pots.

From the experience gained with the DELPHI detectors, the fraction of noisy pixels to be deactivated will be less than  $1 \%$ . Efficiencies per plane including this effect are typically around  $99 \%$  and are always higher than  $95 \%$ .

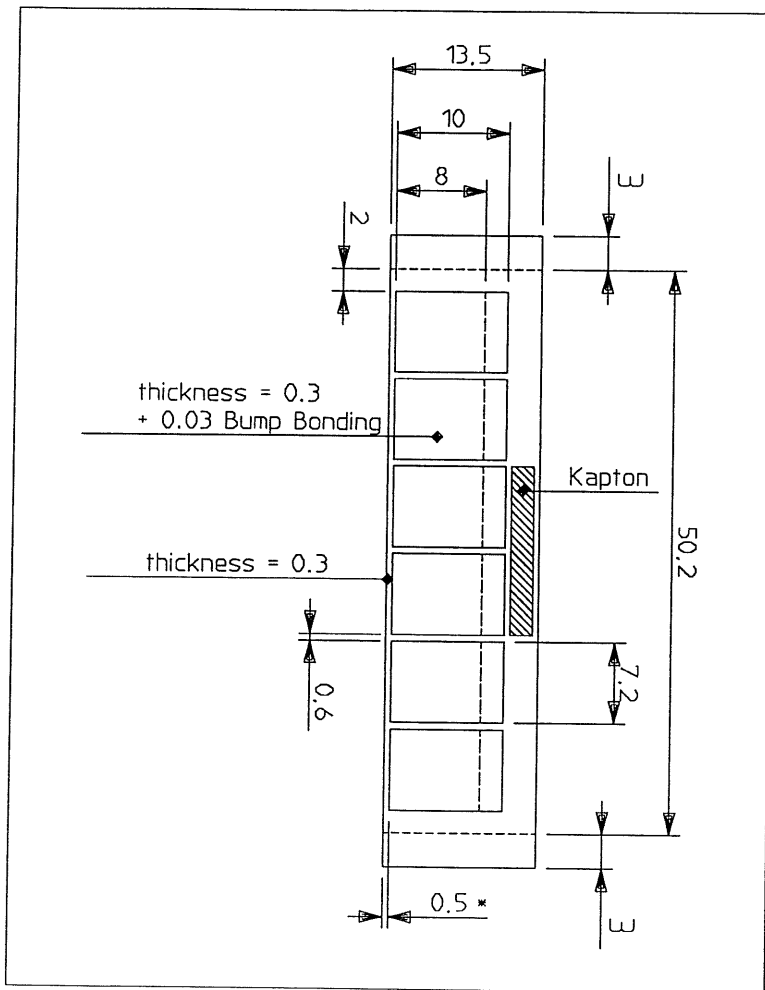


Figure 20: Geometry of a pixel tile with 6 readout chips.

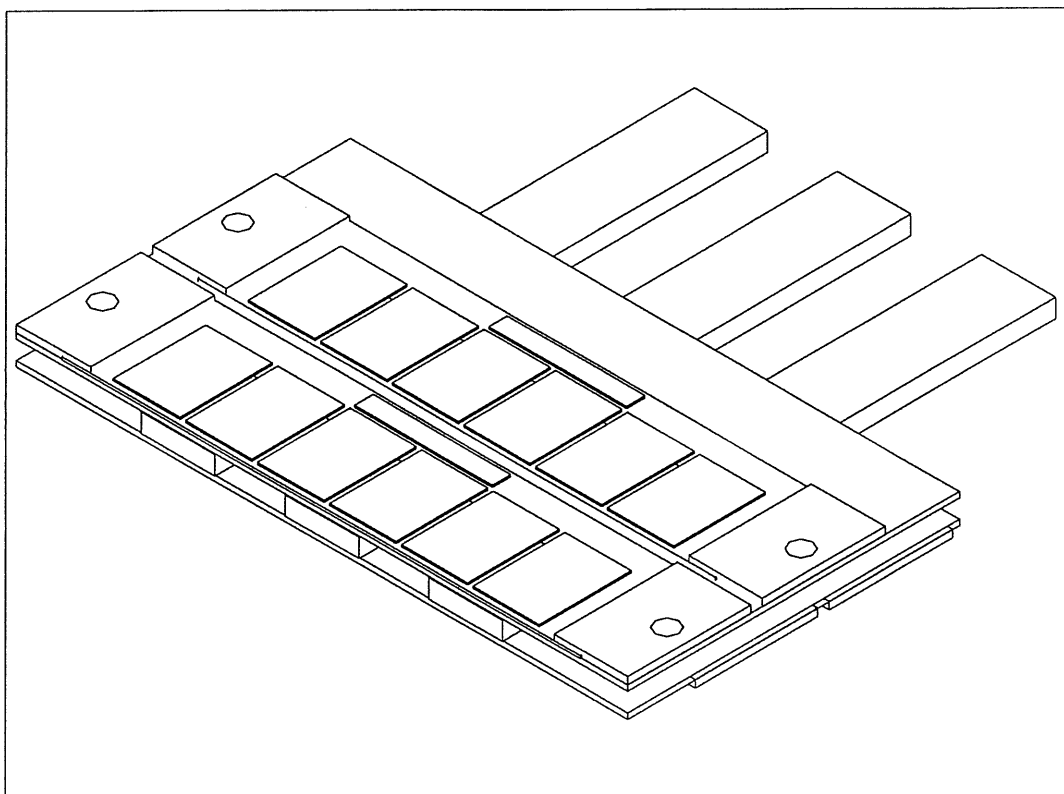


Figure 21: Schematic of a pixel plane with the mechanical support made of three heat pipes between two ceramic planes, each of which supports two pixel tiles.

#### 4.4.2 Mechanical Integration

A 15 mm space is presently left free between the fiber detector planes and the plunger vessel windows. The pixel planes can thus be inserted without removing the fiber detectors.

The pixel planes can be fixed on the present fiber planes fixation holes (see figure 22). This will grant the relative alignment of the fibers and pixel planes and will leave the present global alignment procedures unchanged. With this setup, the distance between two pixel planes is maximal and equal to 10 cm.

The power consumption will be about 1 Watt per pixel tile, providing in total 8 Watts per vertical pot and 4 Watts per horizontal pot. The corresponding heat will be evacuated through the present aluminum support arm. The temperature of the arm will be stabilized below 20°C by implementing an internal water or gas cooling flow. The thermal connection between the pixel planes and the support arm will be of a passive type. In order to avoid a possible damage of the fibers by extreme temperature ( $\geq 50^\circ\text{C}$ ) a monitoring of the pixel planes temperature will be introduced together with an automatic switch off procedure.

First simulations of the proposed setup show thermal inhomogeneities at equilibrium lower than a few  $^\circ\text{C}$ . Possible mechanical angular distortions of the complete 2 pixel planes setup stay below 20  $\mu\text{rad}$ , which has to be compared to the 200  $\mu\text{rad}$  resolution aimed for measurement of the deflection angle with a single pot.

#### 4.4.3 Electronic Integration

The integration of the pixel electronics into the present system will be done at the level of the local electronics crates situated in the HERA tunnel, 10 meters away from the pots. No modification of the present master VME crate configuration will be necessary.

An additional local crate will be added to house the pixels control and readout boards. This crate will be interfaced :

- on the one hand to the pixel planes electronics, through a “repeater board” located on top of each pot in the present electronic box.
- on the other hand to the present local crate housing the fibers digital front-end electronics and managed by the so-called “Crate Controller”.

This second connection will be done at the backplane level and will provide :

- transfer to the pixel electronics of the 3 basic trigger control signals (H1 Clock, Pipe Enable and Fast Clear) and the configuration parameters.
- transfer to the Crate Controller of the encoded pixel hits for a given event.

The present local Crate Controller will have to be slightly upgraded with one more configuration register for the pixel system, and a few more data addresses for pixel readout.

With the proposed setup, changes to the present Roman pots data acquisition system will be minimal. Assuming an efficient latch of noisy cells, the pixel planes are expected to yield not more than an additional few ten words to the present Roman pots data.

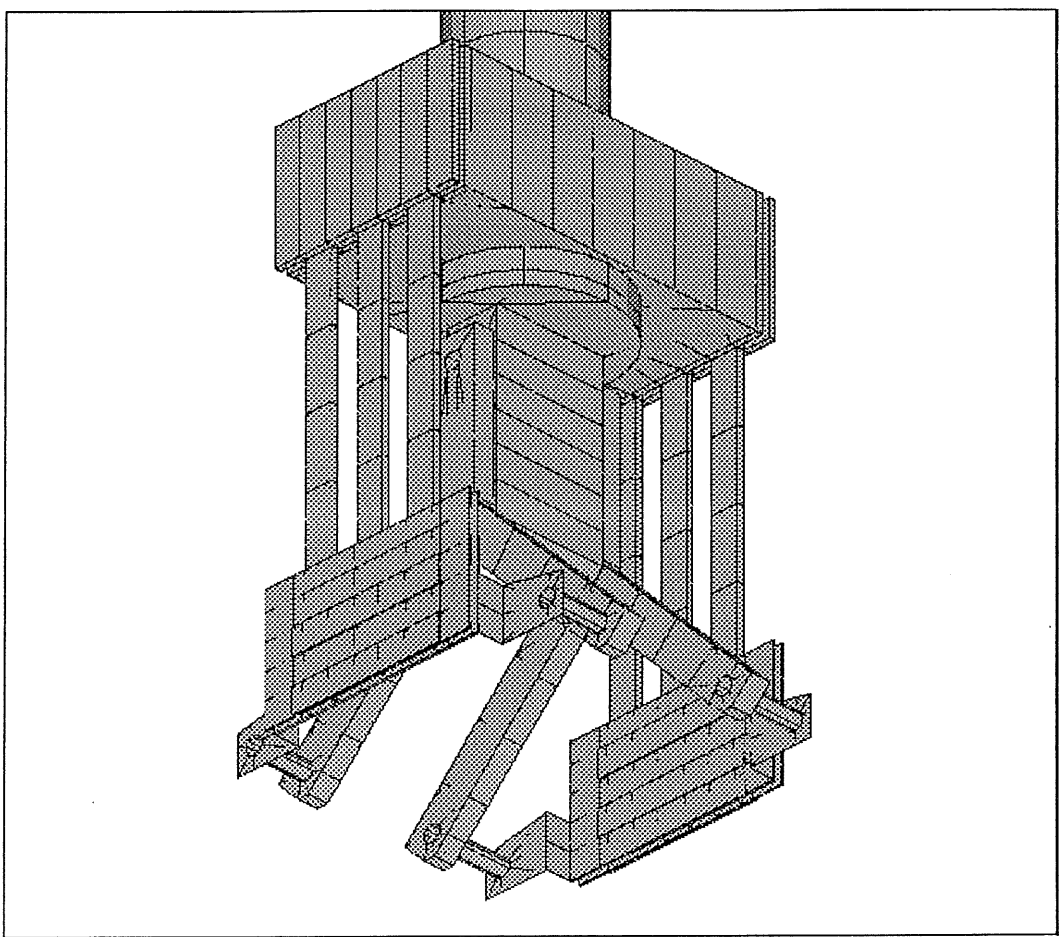


Figure 22: Possible layout of the two pixel planes of a vertical pot mounted on the fiber detector mechanical structure.

## 5 Test Set Up for 1996

The background conditions in the bending plane of the machine may be quite different from the ones above the beam. Therefore H1 will make an effort to install the horizontal Roman pots at 63 and 80 m still during the shutdown 1995/1996 and to mount a set of trigger counters into the new pots to explore the environment.

The time schedule for this installation is extremely tight determined by the delivery time of commercial vacuum components. If the components are ordered in January 1996, an installation date beginning of April could be met. From previous experience with the present set up of vertical pots at 81 and 90 m, where also test measurements with a simple trigger system have been made a year before the final installation, these tests provide extremely useful input to the detector design and pot operation.

## 6 Time Schedule, Responsibilities and Cost

### 6.1 Time Planning for the Horizontal FPS Stations

The time planning aims for an installation into the HERA tunnel during the shut down 1996/1997. According to the experience with the previous installation, which met the anticipated time schedule one year of lead time appears to be sufficient. The following milestone dates are foreseen:

- **January 1996** Complete the design of the vacuum parts, plunger vessels and moving gear.
- **March 1996** Decision on the type of PSPM to be used (Russian or Hamamatsu)
- **March 1996** Complete the design of the fiber hodoscopes and electronics box including cooling.
- **October 1996** Hodoscope tests with the complete electronics chain.
- **February 1997** Installation.

### 6.2 Time Planning for the Installation of Si-Pixel Detectors

The goal is to install the new pixel detectors during the 97-98 shut-down. It is planned to proceed in two steps:

- First step: build a full prototype of a detector tile and of the cooling configuration. This will be based on the readout chip from the current DMILL “MUON” engineering run, and can be ready for autumn 1996. If successful, the prototype tiles can be installed in the 90 m vertical pot for the 1997 data taking period already.
- Second step: full production of the pixel planes and integration within the present system. This can be ready by the end of 1997 for installation during the '97-'98 shut-down.

The most critical aspect of the time planning is the quantification of the DMILL engineering runs, which each induce a delay of about 4 to 6 months.

#### Responsibilities

Vacuum, Survey, Pot mechanics	DESY – Hamburg, Kiel, Prague
Fiber Hodoscopes	DESY – Zeuthen
Readout Electronics	Hamburg II
Data Acquisition	Lebedev Institute

### 6.3 Responsibilities for the Si-Pixel Upgrade

The Marseille group will take responsibility for the pixel mechanics and electronics. The integration within the present system will be made together with DESY-Zeuthen and the Hamburg II Institute, who will provide the necessary changes to the present pots mechanics and electronics.

## 6.4 Cost Estimate for Horizontal Stations

Hodoscopes	50	50
PSPM (Hamamatsu)	160	
PSPM (Dubna)		40
Electronics, cables, trigger	68	100
Mechanics + slow control	60	60
<b>Sum</b>	<b>338 KDM</b>	<b>250 KDM</b>

## 6.5 Cost Estimate for the Si-Pixel Upgrade

Cost estimates are given below. They are based on the conditions obtained when building the DELPHI VFT and the LHC prototypes. They assume conservative production success rates of 50 % for detector substrates (as experienced with the DELPHI VFT) and 20 % for readout chips. Costs of the production phases are not proportional to the respective detector areas because of important offset and quantification effects in the production processes.

In order to reach the target installation date, approval of at least the prototype phase is necessary early 1996.

	Prototype	Production	
		90 m pot option	All pots option
Mechanics	30	60	80
Detector substrates	30	40	40
Readout chips	free	60	120
Bump bonding	40	60	80
External electronics + VME interface	40	50	60
<b>Total</b>	<b>140</b>	<b>270</b>	<b>380</b>

## 7 Summary

The performance of the H1 forward proton spectrometer during the 1995 running period showed that a set up with two stations at 81 and 90 m with scintillating fiber detectors is capable of recording data with the required accuracy for a physics analysis.

The acceptance of the present spectrometer is restricted to large values of the fractional momentum carried by the interacting pomeron in diffractive processes ( $x_{pP} \geq 0.02$ ). In order to reach smaller values it is proposed to add, during the winter shut down 1996/1997, two more detector stations at 63 and 80 m from the interaction point, in which the circulating proton beam is approached sideways. This extension allows to detect protons with momenta close to the incident momentum, which stem from diffractive processes with low mass final states in a kinematic regime, where contributions due to meson exchange are small and only pomeron exchange survives. This extension will thus considerably enlarge the physics scope of the forward spectrometer. There is, however, only little overlap between the kinematic regions covered by

the horizontal part of the spectrometer and the vertical for cross calibration and cross checks. Thus in order to have a bigger redundancy and to improve the performance of the FPS, it is proposed to add high resolution Si-pixel detectors to the existing scintillating fiber hodoscopes.

The largest gain in physics performance is achieved if the 90 m station is upgraded by adding two Si-pixel planes. Due to their good spatial resolution a momentum measurement can be made within the 90 m station alone. As this station is further away from the vertical bending plane than the 81 m station, protons with a higher energy can be detected than with a coincidence requirement between 81 and 90 m. The gain in acceptance covers an interesting regime in  $x_{IP}$  where meson and pomeron exchange both contribute. In addition one benefits from the high detection efficiency of Si-detectors.

To add Si-pixel detectors to all detector stations will improve the momentum resolution of the FPS and increase the detection efficiency.

## References

- [1] W. Hildesheim, M. Seidel, *An Investigation into the Radiation Damage of the Silicon Detectors of the H1-PLUG Calorimeter within the HERA environment*, DESY 95-139.
- [2] A. Staiano ( ZEUS Collaboration ), private communication.
- [3] ATLAS, Technical Proposal, CERN/LHCC/94-43 LNCC/P2.
- [4] DELPHI Collaboration, *Proposal for the upgrade of DELPHI in the forward direction*, CERN/LEPC/92-13.
- [5] L. Blanquart et al., *Test results from prototype pixel chips for ATLAS in DMILL radhard technology*, Proceedings of the first workshop on electronics for LHC experiments, Lisbon, September 11-15 1995, p.68, and CERN/LHCC/95-56.
- [6] M. Dentan et al., *A Mixed Analog-Digital Radiation Hard Technology for High Energy Physics: DMILL ("Durci Mixte sur Isolant Logico-Linéaire")*, CERN/DRDC/92-31 DRDC/P42.
- [7] L. Blanquart et al., *Study of proton radiation effects on analog IC designed for high energy physics in a BiCMOS-JFET radhard SOI technology*, IEEE Trans. Nucl. Sci. vol 41,6 (1994) 2525.
- [8] GEC Marconi Materials Technology Center, Caswell, Towcester UK.
- [9] LETI/ERPC-CENG 85X, F-38041 Grenoble Cedex, France.

## A Comparison with ZEUS<sup>1</sup>

An obvious difference between the ZEUS and the H1 design is the way the circulating beam is approached by the Roman pots. The ZEUS group has decided to approach the beam simultaneously in the horizontal and vertical planes by shaping the bottom of their Roman pots according to the anticipated beam profile. In H1 the bottom of the plunger vessels is flat and two independent pots are necessary to approach the beam horizontally and vertically. By giving up the combined function H1 is independent of the actual shape, size and position of the proton beam paying the price of an extra plunger vessel.

Like ZEUS also H1 relies mainly on twofold coincidences between two stations. To compare acceptances, the acceptance of pairs of FPS stations should be compared. At 81 and 90 m ZEUS is approaching the beam from above and below, while H1 has for financial restrictions only pots, which approach the beam from above, losing about 25% of acceptance. At 63 and 80 m H1 has pots, which move in from the outside of the HERA ring, while ZEUS moves in from both sides gaining about 40% acceptance.

---

<sup>1</sup>Upon the request of the DESY directors a chapter has to be added, where the proposed H1 set up is compared with the ZEUS forward proton spectrometer.

## B Russian Micro-Channel-Plate Photomultiplier

The basic properties of a 100-channel position-sensitive photo-multiplier (PSPM) FEU-2MCP-100<sup>1</sup> have been investigated using light emitting diodes (LED). The LED pulses were tuned to the light yield of a minimum ionizing particle crossing a scintillating fiber of 1 mm diameter. Tests of this PSPM for the readout of scintillating fibers hodoscopes have been performed at the test beam facilities in Serpukhov/Russia and DESY/Germany.

The PSPM has a multi-alkaline photo-cathode with a maximum quantum efficiency of 13 % at 500 nm and 10 % at 430 nm, a fiber optical window and a multiplying system based on two micro-channel plates. A cross section of the PSPM is shown in Fig. 23. The gain at maximum high voltage of 2.8 kV is  $3 \times 10^5$ . The anode matrix consists of  $10 \times 10$  pixels of  $1.5 \times 1.5 \text{ mm}^2$  size.

Illuminating all PSPM channels by LED pulses via a 1 mm fiber the sensitivity and the cross talk have been measured. The frequency dependence of the amplitudes up to 1 MHz and the long time behavior of the PSPM under conditions of the Forward Proton Spectrometer have been investigated. The following results were obtained:

- the mean detection efficiency in the light regime of 15 photons, i.e. 1.5 - 2.0 photoelectrons, is 70 % for blue fibers and 60 % for the green ones;
- the crosstalk is less than 1.5 % for all PSPM channels;
- for pulse rates up to 10 kHz per PSPM channel the amplitudes show no significant degradation, while above this value a considerable reduction was observed – the efficiency loss is however only a few percent up to rates around 100 kHz per channel;
- the operation of the PSPM during one month at the pulse rate of 50 kHz per channel showed a 20 % degradation of the amplitudes at the first stage and a stable response in the following stage;

In a more realistic application the PSPM was used as a readout device for multi-layer fiber detectors coupled by a special mask to the photo-cathode of the PSPM. All fiber detectors were delivered by the DESY-Zeuthen group. One fiber detector consists of 8 layers of 12 fibers of 1 mm diameter emitting blue/green photons. The fiber layers were staggered to each other by 0.25 mm. The second fiber detector consists of 0.5 mm blue scintillating fibers arranged in 8 layers per 16 fibers staggered by 0.125 mm relative to each other.

Cosmic particles, beam dump muons and 5 GeV electrons were used to investigate the tracking properties of the combined system fiber detector plus PSPM. The following results were obtained:

- the internal resolution is about 100  $\mu\text{m}$  and 70  $\mu\text{m}$  for the detectors consisting of 1mm and 0.5 mm fibers, respectively;
- the mean detection efficiency per fiber layer is 60-65 % for 1 mm blue fibers, 50-55% for 1 mm green fibers and about 45 % for 0.5 mm blue fibers at the high voltage of 2.8 kV; the dependence of the efficiency on the high voltage is shown in Fig. 24;

---

<sup>1</sup>producer Moscow Electrolamp Factory

According to the presented results this type of PSPM is a suitable readout device for the scintillating fiber detectors which are foreseen in the horizontal Roman pots of the H1 Forward Proton Spectrometer. A modified version of the PSPM is now in preparation<sup>2</sup>. The quantum efficiency in the blue light region (at 430 nm) should be increased up to 15 % and the number of anode channels will be enlarged up to 132 by an optimum coverage of the whole sensitive area of the micro-channel plates. Two exemplars of the modified PSPM should be ready in January 1996.

<sup>2</sup>producer Moscow Electrolamp Factory

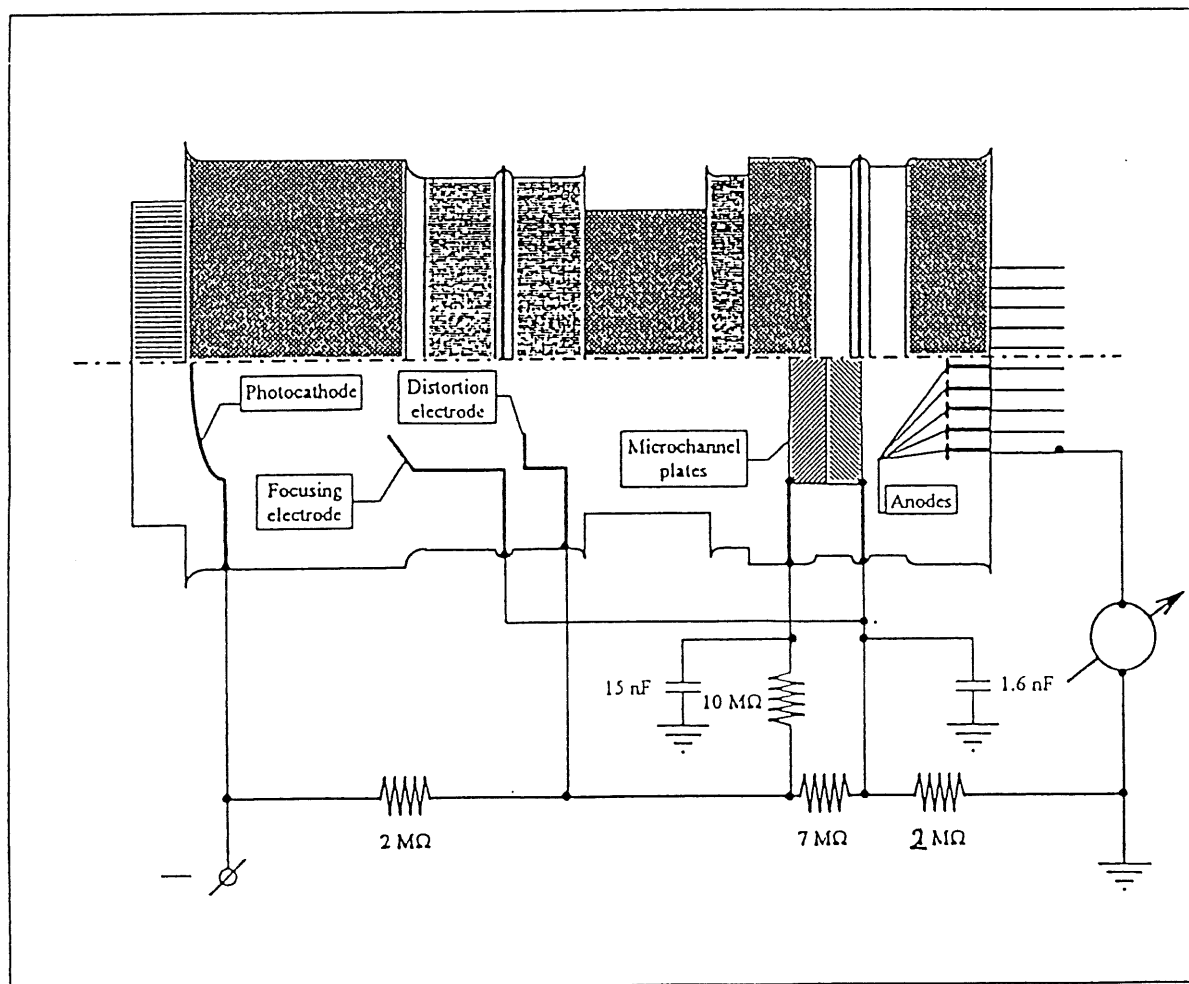


Figure 23: Schematic layout of the Micro-Channel-Plate photomultiplier.

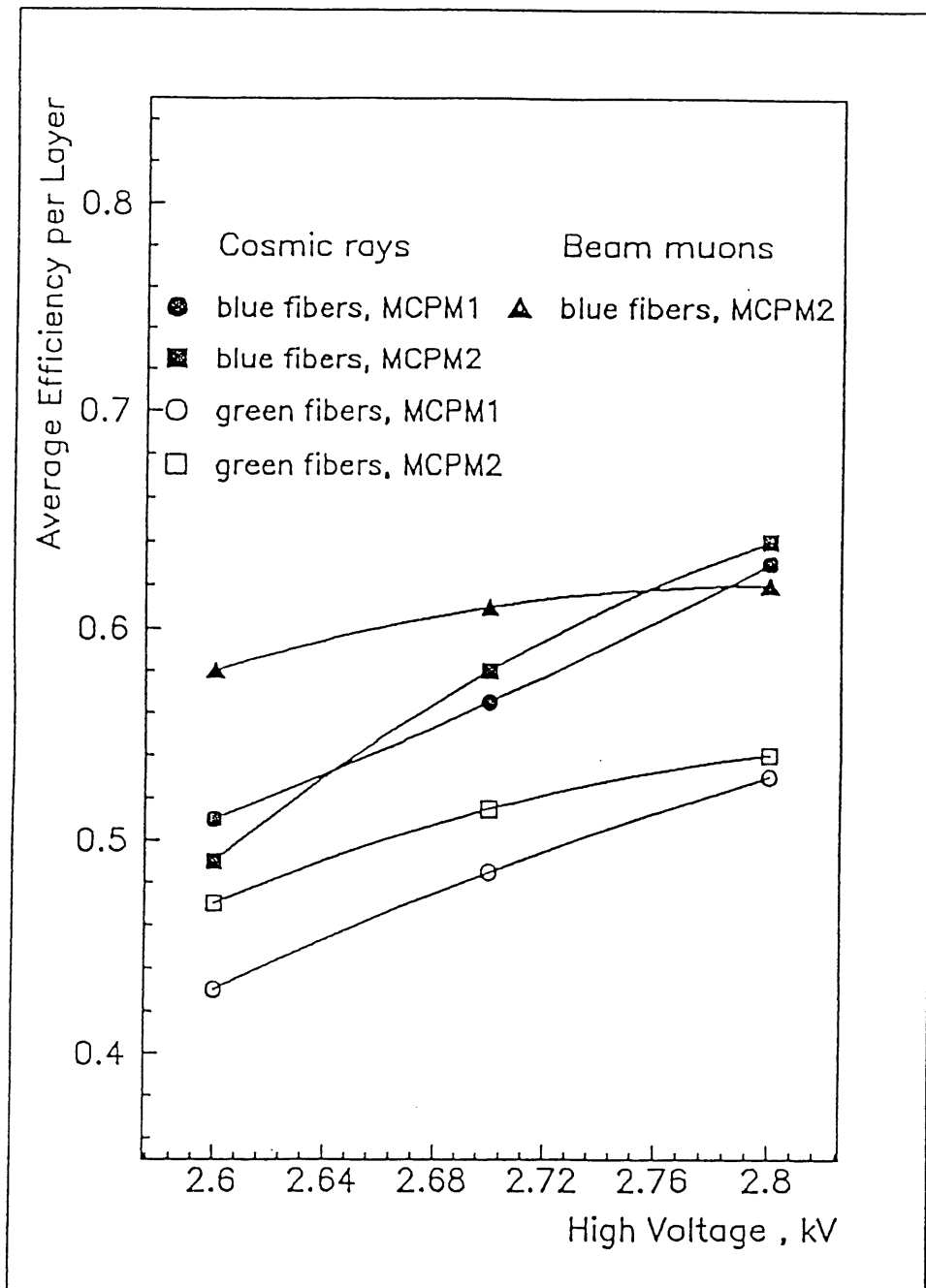


Figure 24: Mean detection efficiency per fiber layer as function of high voltage.